Constraining topsoil pesticide degradation in a conceptual distributed catchment model with compound-specific isotope analysis (CSIA)

Sylvain Payraudeau[1], Pablo Alvarez-Zaldivar[1], Paul van Dijk[2], Gwenaël Imfeld[1]

[1]Institut Terre et Environnement de Strasbourg, Université de Strasbourg, CNRS/ENGEES, ITES UMR 7063, Strasbourg, 67084, France

[2]Chambre Régionale d'Agriculture Grand Est, Espace Européen de l'Entreprise, 2 rue de Rome CS 30022 Schiltigheim, 67013 France

Correspondence to: Sylvain Payraudeau (sylvain.payraudeau@engees.unistra.fr)

Abstract. Predicting pesticide dissipation at the catchment scale using hydrological models is challenging due to limited field data distinguishing degradative from non-degradative processes. This limitation hampers the calibration of key parameters such as biodegradation and volatilization half-lives (DT_{50}), and the carbon-water partition coefficient (K_{oc}), often leading to equifinality and reducing confidence in predictions of pesticide persistence in topsoil and transport from agricultural field to catchment outlets. This study examines the use of pesticide Compound-Specific Isotope Analysis (CSIA) data to improve model predictions of pesticide persistence in topsoil and off-site transport at the catchment scale. The study was conducted in a 47-ha crop catchment using the pre-emergence herbicide S-metolachlor. A new conceptual distributed hydrological model, PIBEACH, was developed to simulate daily pesticide dissipation in soils and its transport to surface waters. The model integrates changes in the carbon isotopic signatures ($\delta^{13}C$) of S-metolachlor during degradation to constrain key parameters and reduce equifinality. Model and parameter uncertainties were estimated using the Generalized Likelihood Uncertainty Estimation (GLUE) method. Incorporating $\delta^{13}C$ data and S-metolachlor concentrations from topsoil samples reduced the uncertainty in the estimated degradation half-life DT_{50} by more than half, yielding a value of 18 ± 4 days. This approach also significantly decreased uncertainty in six key metrics of pesticide persistence and transport. Between the day of application (day 0) and day 115, the modelled mass balance components, ranked by relative contribution, were as follows: degradation accounted for the majority at $82 \pm 21\%$, followed by the remaining bioavailable mass in the topsoil at $12 \pm 8\%$. Leaching contributed $4 \pm 17\%$, while export to the river outlet accounted for $2 \pm 6\%$. The irreversibly sorbed mass represented $1.1 \pm 2.0\%$, and volatilization was minimal ($<1\%$). The results highlighted that moderate, targeted sampling effort can identify degradation hot-spots and hot-moments in agricultural soil when stable isotope fractionation is integrated into the model. Overall, integrating CSIA data into PiBEACH model significantly enhances the reliability of pesticide degradation predictions at the catchment scale. In addition, PiBEACH, which accounts for spatial and seasonal variations in topsoil pesticide concentrations, enables coupling with distributed, event-based hydrological models such as OpenLISEM OLP to capture intra-event pesticide transport dynamics more accurately.

1 Introduction

Ongoing intensive use of pesticides can lead to accumulation of pesticides and their transformation products in agricultural soils, and pesticide off-site transport for decades. Pesticides on agricultural soil can be mobilized and transported off-site towards aquatic ecosystems during rainfall-runoff events, thereby threatening drinking water supply as well as ecosystem and human health (Vorosmarty et al., 2010; Fenner et al., 2013; Stone et al., 2014; Weisner et al., 2021). While pressure on aquatic ecosystems continues to increase, accurately quantifying and predicting the contribution of individual pesticide dissipation processes in soil, through degradation and off-site transport to the catchment outlet, remains a major challenge. In this context, reliable and validated hydrological models that predict pesticide dissipation and off-site transport have the potential to address fundamental questions, such as the relationship between hydro-climatic factors and pesticide dissipation processes with respects to the transfer risks of pesticides on the catchment scale. The contribution of degradative processes, including both biotic or abiotic degradation, as well as non-degradative pesticide dissipation processes, such as sorption, leaching, volatilization and off-site transport, must be quantified for this purpose in models (Larsbo and Jarvis, 2005; Steffens et al., 2015; Gassmann, 2021). The accurate and sufficiently precise prediction of pesticide dissipation and off-site transport on the agricultural catchment scale raises, however, two fundamental limits. First, the complexity of reactive transport models has increased over the last decade while field datasets available to calibrate and validate such models remain scarce (Medici et al., 2012; Ammann et al., 2020). In addition, existing models frequently fail to accurately quantify the contribution of concomitant pesticide dissipation processes for accurate estimation of off-site pesticide transport (Gassmann et al., 2021).

Model prediction of pesticide dissipation and off-site transport towards aquatic ecosystems generally suffers from field data limitations to constrain model parameters by calibration. Conceptual and physically-based hydrological models account for many dissipation and transport phenomena, each of which generally accounts for several physico-chemical processes and described by several parameters obtained in reference laboratory experiments (Gatel et al., 2020; Gassmann, 2021). Linking pesticide dissipation parameters obtained under laboratory conditions with field processes is however difficult, because the extent and the range of values for a given parameter may differ under laboratory and field conditions (Malone et al., 2004; Köhne et al., 2009). As a result, parameter calibration is often required to fit observations. For instance, pesticide half-life (DT_{50}) in soil, i.e., the time required for 50 % dissipation of the parent compound in soil, is typically derived under laboratory conditions (Lewis et al., 2016). However, when extrapolated to field conditions, other process-controlling parameters, including soil moisture, temperature, K_{OC}, organic carbon content and porosity distribution, affect pesticide concentrations (Dubus et al., 2003). As a result, DT_{50} values obtained from literature typically span up to one order of magnitude (Lewis et al., 2016; Wang et al., 2018). Pesticide half-life is thus generally considered as a lumped calibration parameter in reactive transport models (Dubus et al., 2002), merging both degradative and non-degradative pesticide dissipation processes across different soil components and redox conditions (Honti and Fenner, 2015). As a result, reducing uncertainty in DT_{50} values

remains challenging at the catchment scale, despite being crucial for improving the predictive accuracy of pesticide transport models that can serve water quality management.

65

Pesticide concentrations in topsoil and in river at the catchment outlet are currently the most accessible information for modelling pesticide reactive transport at the catchment scale (Wendell et al., 2024). In the best of cases, calibration is carried out based on concentrations of both parent and main transformation products in soil, runoff or aquifer (Gassmann, 2021), which improved model prediction (Sidoli et al., 2016; Lefrancq et al., 2018). Transformation products, however, are typically

70 numerous, several of them are unknown and possibly further degraded, which may lead to incomplete and uncertain mass balance accounts. As a result, pesticide and transformation product concentration data often provide limited insight into distinguishing degradative from non-degradative dissipation processes in catchments (Fenner et al., 2013). Consequently, existing models struggle to differentiate between competing dissipation processes and to quantify their respective contributions.

75

Evaluating pesticide dissipation processes in field is essential as degradation is the only process that reduces the total pesticide load in environmental compartments. While degradation limits long-term pesticide accumulation, it may also produce unknown and potentially toxic transformation products that can be transported to surface and groundwater. In this context, pesticide compound specific isotope analysis (CSIA) offers an alternative approach, as it infers degradation independently of

80 concentration data and transformation product identification, relying instead on changes in stable isotope ratios (Elsner and Imfeld, 2016; Hofstetter et al., 2024). During pesticide degradation, lighter isotopes (e.g., ^{12}C) typically react slightly faster than heavier ones (e.g., ^{13}C), producing a kinetic isotope effect. This effect creates a distinct isotopic signature, reflected in changes in the isotope ratios of degrading molecules (Elsner, 2010). The stable isotope fractionation (ε_{lab}, e.g., for carbon) can be determined through closed-system microcosm experiments and applied under specific conditions to quantify pesticide

85 degradation under field conditions (Alvarez-Zaldivar et al., 2018). In contrast, non-destructive processes like dispersion and sorption are not expected to induce significant isotope fractionation under agricultural field conditions (Eckert et al., 2013; van Breukelen and Prommer, 2008; van Breukelen and Rolle, 2012; Kopinke et al., 2017). Hence, incorporating pesticide CSIA data into hydrological models can reduce uncertainties in pesticide dissipation processes by distinguishing between degradative and non-degradative processes, as well as transformation pathways. Such uncertainties may arise from compensatory effects

90 among overlapping dissipation processes, as previously demonstrated for legacy contaminants in aquifers (Hunkeler et al., 2008; Blázquez-Pallí et al., 2019; Thouement et al., 2019; Antelmi et al., 2021; Prieto-Espinoza et al., 2021) and wetlands (Alvarez-Zaldivar et al., 2016).

More recently, CSIA data have been integrated into a lumped transport model using travel time distributions, enhancing the

95 interpretation of pesticide transport and transformation processes at the catchment scale (Lutz et al., 2017). However, lumped models primarily capture aggregate hydrological behaviour with some applications in water quality such as nitrate trends

(Broers et al., 2024) but they do not account for spatial variability in landuse or in topsoil parameters, including soil moisture and soil temperature (Fatichi et al., 2016). This limitation restricts their ability to represent landscape heterogeneity, such as variations in crop distribution and pesticide applications, thereby impeding the accurate identification of contaminant sources and degradation hotspots (Grundmann et al., 2007). In contrast, distributed conceptual and physically-based models explicitly represent spatially distributed hydro-climatic dynamics regulating hydrological processes, such as runoff and infiltration. Yet, pesticide CSIA data have not been integrated into the calibration and validation of such models due to the lack of suitable field datasets. Moreover, the limited availability of information on the initial isotopic composition of commercial pesticide formulations has constrained the broader application of CSIA. This limitation has recently been addressed by ISOTOPEST, a database compiling the isotopic signatures of commercial formulations to support the use of CSIA in pesticide studies (Masbou et al., 2024).

This study aimed to evaluate the benefits of using both topsoil pesticide concentrations and CSIA data for calibrating a distributed hydrological model to quantify pesticide dissipation and off-site pesticide transport at the catchment scale. The study relied on a unique field dataset comprising weekly measurements of S-metolachlor concentrations and carbon isotope ratios (δ^{13}C) in soil and runoff from a 47-hectare agricultural headwater catchment located in Alsace, France (Alvarez-Zaldivar et al., 2018). To capture hydro-climatic effects on pesticide degradation, drawing upon previous work by Boesten and Vanderlinden (1991), Schroll et al. (2006) and Gassmann (2021), we adapted the Bridge Event And Continuous Hydrological (BEACH) distributed conceptual model, originally developed for soil water dynamics (Sheikh et al., 2009). This adaptation led to the development of PiBEACH (Pesticide isotope BEACH), extending the lumped isotope modeling approach of Lutz et al. (2017) into a spatially distributed framework. Model calibration and uncertainty analysis were performed using the Generalized Likelihood Uncertainty Estimation (GLUE) approach. This allowed us to evaluate how the inclusion of CSIA data improved model predictions and parameter identifiability, particularly in representing pesticide degradation across heterogeneous catchment conditions.

2 Material and Methods

2.1 Field site

The dataset, including concentrations and carbon isotope signatures ($\delta^{13}C$) of S-metolachlor in soil, was collected from March 19th (day 0) to July 12th (day 115), 2016 from the 47-ha Alteckendorf headwater catchment (Bas-Rhin, France; 48 47 19.56 N; 7 35 2.27 E) (Alvarez-Zaldivar et al., 2018; Lefrancq et al., 2018) (Fig. 1).

Figure 1: The Alteckendorf headwater catchment (Bas-Rhin, France), showing the experimental setup, including three transects, i.e. North, Valley and South (weighted samples collected at green dots along red lines) and plot sampling (black dots). Land use for 2016 is also displayed. The "Other" category includes roads, grass strips and orchards.

130

Daily temperature and potential evapotranspiration were obtained from the MétéoFrance station in Waltenheim-sur-Zorn, located 7 km southwest of the study site. Daily rainfall was measured using a tipping bucket rain gauge (Précis Mécanique®, Fig. 1). Detailed climate and hydrological data are provided in Table S1. The catchment is predominantly arable land, with corn (18 %), sugar beet (70 %) and wheat (3 %) as the main crops in 2016. A subsurface tile drainage system, of unknown spatial extent, is present at a depth of 0.8 m depth. Water is collected via ditches and discharged through a 50 cm diameter pipe at the catchment outlet (Fig. 1). Soils are classified as Haplic Cambisol Calcaric Siltic and Cambisol Eutric Siltic on hillsides (north and south), and Cambisol Colluvic Eutric Siltic in the central valley. Soil analysis from 48 topsoil samples (0-20 cm) and six 2 m depth profiles showed low spatial variability across the catchment (Lefrancq et al., 2018). Texture is predominantly composed of silt (61.0 ± 4.5 %), followed by clay (30.8 ± 3.9 %) and sand (8.5 ± 4.2 %). The soil also contains calcium carbonate ($CaCO_3$: 1.1 ± 1.6 %), organic matter (2.2 ± 0.3 %), total soluble phosphorus (0.11 ± 0.04 g kg^{-1}), and cation exchange capacity (CEC: 15.5 ± 1.3 cmol kg^{-1}). Soil pH averaged 6.7 ± 0.8 (n = 30). A compacted plough layer was observed between 20 and 30 cm depth. In 2016, S-metolachlor was applied to corn and sugar beet plots in three applications: March 20-25, April 13-14 and May 25-31. These plots covered 88 % of the catchment area. Application dates, doses and formulation

were obtained for each plot from farmer surveys, providing spatially distributed data for modelling. In total, 20.2 kg, 5.9 kg,
145 and 14.0 kg of S-metolachlor were applied to the North, Valley, and South transects, respectively (Table S2).

2.2 Soil and water sampling and outlet discharge measurements

Samples from the topsoil (0-1 cm) were collected from individual plots and upstream-downstream transects across the catchment (Fig. 1 and S1; Alvarez-Zaldivar et al., 2018). Thirteen marked plots were sampled before S-metolachlor application
150 and on days 1, 50, and 100 after application. In addition, weekly weighted composite samples were taken along the north, valley, and south transects (green dots in Fig. 1) from March 19 (day 0) to July 12 (day 115). All soil samples were analysed for S-metolachlor concentration and carbon isotope composition ($\delta^{13}C$) using CSIA. The volumetric topsoil water content (m^3_{water} m^{-3}_{soil}) was calculated from gravimetric measurements after drying samples at 110°C following NF ISO 1146 (Lefrancq et al., 2018). This procedure was applied to all samples, including field samples collected on days 1, 50 and 100 after
155 application, as well as the weekly mixed samples from the three transects. It incorporated seasonal variations in topsoil bulk density, as modelled by PiBEACH and detailed in the Supplement, Section 7.2.

Runoff discharge at the catchment outlet was measured using a Doppler flowmeter (2150 Isco) with 3% accuracy and a 2 min resolution. Continuous, refrigerated, flow-proportional sampling was carried out using an Isco Avalanche autosampler
160 equipped with twelve 330 mL bottles. Samples were collected based on fixed weekly discharge volumes from 50 to 150 m^3, in order to capture progressive increase in baseflow discharges from April to June 2016 (Alvarez-Zaldivar et al., 2018). To obtain sufficient S-metolachlor for quantification and CSIA, weekly composite samples were prepared by pooling bottles according to hydrograph phase (base-flow, rising limb, and falling limb), yielding one to four samples per week with volumes ≥ 990 mL (Alvarez-Zaldivar et al., 2018). Piezometric monitoring of the shallow aquifer was not possible due to the absence
165 of observation wells at the study site.

2.3 S-metolachlor quantification and δ¹³C analysis

To separate dissolved and particulate phases of S-metolachlor, river water samples were filtered through 0.7 µm glass fibre filters. Extraction of S-metolachor from soil and water samples was performed using an AutoTrace 280 Solid Phase Extraction (SPE) system (Dionex) with SolEx C18 cartridges (Dionex ®), as previously described (Alvarez-Zaldivar et al., 2018; Gilevska
170 et al., 2022). Quantification was carried out using chromatography–mass spectrometry (GC-MS, ISQ™, Thermo Fisher 173 Scientific). Quantification limits were 0.01 µg L^{-1} for water and 0.001 µg g^{-1} (dry weight) for soil and suspended matter, with a total analytical uncertainty of 8 % and 16 %, respectively. Carbon isotope ratios ($\delta^{13}C$) of S-metolachlor in soil and water were analysed using a GC-C-IRMS, comprising a TRACE™ Ultra gas chromatograph (ThermoFisher Scientific) coupled to a Delta V plus isotope ratio mass spectrometer via a GC IsoLink/ Conflow IV interface (Alvarez-Zaldivar et al., 2018; Gilevska
175 et al., 2022b; see also Section 5, Supplement). The reproducibility of triplicate δ¹³C measurements was ≤0.2‰ (1σ). A

minimum peak amplitude of 300 mV, corresponding to approximately 10 ng of carbon injected on column, was required for accurate isotope analysis.

2.4 PiBEACH model description

PiBEACH development. The Pesticide-isotopes BEACH model (PiBEACH) was developed in Python based on the conceptual
180 Bridge Event And Continuous Hydrological (BEACH) model (Sheikh et al., 2009). BEACH was chosen for its demonstrated ability to simulate daily topsoil moisture and catchment discharge with high accuracy (Nash-Sutcliffe efficiency of 0.79) in a 42 ha catchment (Sheikh et al., 2009) with loess soils and crops similar to those observed in the study catchment. BEACH is a grid-based model that simulates spatially distributed soil water content and catchment outlet discharge by accounting for key hydrological processes, including evaporation, plant transpiration, percolation, deep percolation, lateral flow and runoff
185 (Sheikh et al., 2009). Similar to BEACH, the PiBEACH model employs square cells (x, y) with variable depths (z) corresponding to the soil layers considered (Fig. 2), in order to represent water and pesticide movement within the catchment, as detailed below. At the cell scale, daily vertical water fluxes are computed across soil layers, followed by lateral fluxes upstream to downstream. Surface flow direction is derived from the digital elevation model using flow-accumulation functions, without employing a numerical scheme (Sheikh et al., 2009).
190 The model is driven by daily meteorological records (rainfall, air temperature and potential evaporation), soil physical properties (saturated hydraulic conductivity, bulk density, porosity, both for the plow layer and a deeper soil layer), and crop-specific agronomical parameters. PiBEACH extends BEACH by incorporating experimental knowledge of hydrological and pesticide transport processes observed in the Alteckendorf catchment (Lefrancq et al., 2017; Lutz et al., 2017; Alvarez-Zaldivar et al., 2018; Lange et al., 2018; Lefrancq et al., 2018). It translates the perceptual model developed by field researchers into a
195 conceptual framework, following the approach of Ammann et al. (2020).

Key modifications in PiBEACH include: (i) a topsoil mixing layer, assuming that pesticide transport is controlled by a mixing layer from 0.25 to 2 cm below the soil surface, in which rainfall, soil solution and runoff are assumed to mix instantaneously (McGrath et al., 2008), and deeper soil layers to capture groundwater contributions to discharge, (ii) daily simulation of topsoil temperature (Neitsch et al., 2011), (iii) daily dynamic topsoil hydraulic properties that reflect crop-specific agronomical
200 practices (Lefrancq et al., 2018), (iv) first-order pesticides degradation and linear sorption/desorption, and (v) pesticide carbon stable isotopic fractionation and transport of bulk heavy and light carbon in the pesticide molecule (e.g., ^{13}C and ^{12}C) (Lutz et al., 2017; Alvarez-Zaldivar et al., 2018). PiBEACH requires spatially explicit inputs of pesticide application dates and quantities for each plot.

205 *Comparison of PiBEACH with physically-based models.* The finite difference or finite volume method is typically used to simulate agricultural catchment hydrology in 3D physically-based models, e.g., Hydrogeosphere (De Schepper et al., 2015) or CATHY (Gatel et al., 2020). However, modelling pesticide reactive transport including pesticide sorption-desorption and degradation on the catchment scale remains challenging. This challenge arises because numerical dispersion can affect the

mass balance at the catchment scale (Gatel et al., 2020) to an extent comparable to the pesticide export coefficient, defined as the ratio of the mass transported at the outlet to the total mass applied within the catchment, which typically ranges from 0.1‰ to 1% of the applied pesticide load (Lefrancq et al., 2018).

The numerical dispersion issues can be mitigated, though this leads to longer computation times in both 2D (Lutz et al., 2013) and 3D (Gatel et al., 2020) models. PiBEACH simulates water and pesticide fluxes on a daily time step, tracking flow from upstream to downstream along branches of the drainage network using flow-accumulation grid-based functions (Sheikh et al., 2009). While it avoids numerical issues by not employing differential equations and associated numerical schemes, this approach also limits its ability to predict fast flow dynamics, i.e., runoff genesis and preferential water flow. The drainage network can be extracted from a LIDAR digital elevation model (Lefrancq et al., 2017). A vertical mass balance is computed using the sum of discharges and pesticides masses of the upstream grid cells as lateral inputs for the downstream grid cells (section 6 of the SI and equation 2). The daily resolution of PiBEACH reduced by one to two orders of magnitude lower the computation time compared to 2D or 3D models for catchments of similar size (Gatel et al., 2020). The limitations associated with this conceptual approach are discussed in the next section.

PiBEACH description and sub-model components. To account for landscape features affecting pesticide off-site transport, such as grass strips or roads, the Alteckendorf catchment was modelled using a 2×2 m raster resolution. The vertical soil profile was divided into five successive layers from the topsoil to the groundwater (Fig. 2): (i) a surface mixing layer (z_0: 0-1 cm) (McGrath et al., 2008), (ii) a plow layer observed in the field (z_1: 1-30 cm), (iii) a drainage layer controlled by tile drains, as observed in the Alteckendorf catchment (z_2: 30-80 cm), (iv) a variably saturated layer (z_3), and (v) a permanently saturated groundwater layer (z_4). The combined groundwater depths ($z_3 + z_4$) varied spatially and seasonally across the catchment, with a maximum observed depth of 23.2 m, consistent with recharge dynamics in monitored hillslopes (Molenat et al., 2005). The partitioning between z_3 and z_4 was defined as a calibration parameter z_f, such that if $z_3 + z_4 = 23.2$ m; $z_3 = 23.2 \times z_f$; $z_4 = 23.2 \times (1 - z_f)$ (Table S3 in Supplement).

The hydrological balance follows the formulation of Sheikh et al., (2009), with process-specific implementations detailed in Section 6 of the Supplement. For each grid cell i of each soil layer zj, the daily change in volumetric soil water content (θ, m³ m⁻³) is calculated using:

$$\Delta \theta_i = R_{i,zj} - RO_{i,zj} + \Delta LF_{i,zj} - Ea_{i,zj} - Ta_{i-zj} - P_{i,zj} \qquad (1)$$

where daily rainfall (R), runoff (RO) (calculated for z_0), net cell lateral inflow-outflow (ΔLF), actual evaporation (Ea), actual transpiration (Ta) and percolation (P) were expressed in mm H_2O d⁻¹. Four layers, z_0 to z_3 where concerned by equation 1. Evaporation (Ea) affects layers z_0 to z_3, while transpiration (Ta) depends on plant root depth following crop-specific development stages (see sections 6.5 and 6.6 in the Supplement). Lateral flow (ΔLF) and percolation (P) are calculated from

upstream to downstream cells for layers z_0 to z_3 (Manfreda et al., 2005). Percolation across the saturated layer z_4 is routed to the outlet as a global linear reservoir (Manfreda et al., 2005).
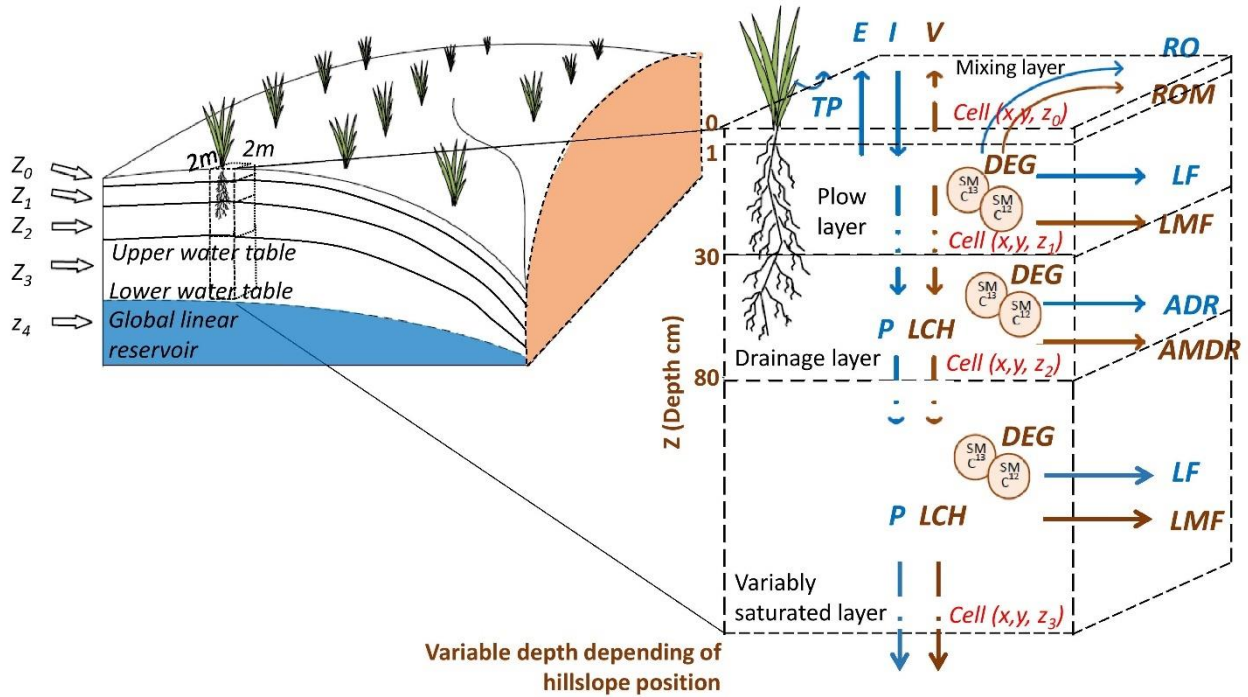
Figure 2: Conceptual representation of the five-layer (z_0 to z_4), spatially distributed hydrological and reactive transport model
245 PiBEACH, employing a 2 × 2 m raster resolution and variable depths depending on soil layers, from z_0 to z_3. Hydrological processes include evaporation (*E*), transpiration (*TP*), percolation (*P*), volatilization (*V*), runoff (*RO*), lateral flow (*LF*), and artificial drainage (*ADR*). Pesticide mass transfer processes include volatilization (*V*), runoff mass (*ROM*), lateral mass flow (*LMF*), leaching (*LCH*), mass transfer via artificial drainage (*AMDR*), and degradation (*DEG*) with isotope fractionation (*SM ^{13}C* and *SM ^{12}C*).

250

The agronomical sub-model of PiBEACH (Lefrancq et al., 2017) (see Supplement, Section 7) simulates seasonal variation of in topsoil soil hydraulic properties, improving the hydrological balance of the headwater catchment (Lefrancq et al., 2017). The pesticide dissipation sub-model of PiBEACH represents the key processes governing pesticide reactive transport at the catchment scale (Fig. 2). The pesticide mass (*M*, g) balance for each cell *i* and each layer is expressed as:

255
$$\frac{dM_i}{dt} = A_i - ROM_i + \Delta LMF_i - V_i - LCH_i - DEG_i \tag{2}$$

where *M* is the pesticide mass (g), *A* is the applied mass (g d^{-1}), *ROM* is mass lost via runoff (z_0 only), *ΔLMF* is lateral mass flow (z_0–z_3), *V* is volatilization (z_0), *LCH* is leaching (z_0–z_3), and *DEG* is degradation (z_0–z_4).

Pesticide partitioning into dissolved, sorbed and gaseous phases follows Leistra et al., (2001) (see Supplement Section 8). Partition into the dissolved and adsorbed phases was determined by linear sorption, considering the organic carbon-water partition coefficient K_{OC} (mL g^{-1}) normalized by the fraction of organic carbon f_{OC} (kg kg^{-1}) in soil, where the pesticide dissociation coefficient (K_d, mL g^{-1}) was given by $K_d = K_{OC} \times f_{OC}$. Partitioning into the gas phase was obtained from the dimensionless Henry constant, $K_H^{cc} = 9.55\ 10^{-5}$ for S-Metolachlor (Feigenbrugel et al., 2004). General pesticide mass flux J (µg d^{-1}) for each model cell is computed as:

$$J = q_{x,y} \times C_{aq} \tag{3}$$

where $q_{x,y}$ is the water flux vector (mm d^{-1}) in the lateral (x, y) direction and C_{aq} is the dissolved S-metolachlor concentration in the aqueous phase (µg mm^{-1}). In the topsoil layer (z_0), runoff and volatilization are included:

$$J_{zo} = q_{x,y} + c_{aq} \left(RO e^{-\beta_{RO} D_{zo}} + \frac{1}{r_a + r_s} \right) \tag{4}$$

where RO is runoff (mm), β_{RO} is a calibration constant ($1 \geq \beta_{RO} \geq 0$) and D_{z0} (mm) is the mixing layer depth (Ahuja and Lehman, 1983). Volatilization was limited to the first 5 days after application (Gish et al., 2011), (Prueger et al., 2005), and follows (Leistra et al., 2001), with fluxes across topsoil controlled by air transport resistance, r_a, (d m^{-1}) and diffusion resistance, r_s (d m^{-1}) (Leistra et al., 2001) (see sub-section 8.2 of the Supplement).

Biodegradation occurs only in bioavailable fractions of adsorbed (*ads*) and aqueous (*aq*) phases (Thullner et al., 2013). A similar stable isotope fractionation associated with degradation was then considered for the bioavailable fractions, including the adsorbed (Eq. 5, second term) and the aqueous (Eq. 6) phases. The bioavailable fraction was controlled kinetically by an ageing rate k_{age} (d^{-1}) on the adsorbed fraction (Schwarzenbach, 2003). Due to the physicochemical properties of S-metolachlor, abiotic degradation processes such as photolysis, and their associated isotope fractionation, were excluded from the model. While non-destructive processes like dispersion and sorption may induce isotope fractionation under conditions of strong sorption behavior, transient diffusion, or repeated sorption–desorption cycles (Eckert et al., 2013; van Breukelen and Prommer, 2008; van Breukelen and Rolle, 2012; Kopinke et al., 2017), these effects were considered negligible. Given the rapid biodegradation of S-metolachlor in soil and the limited impact of sorption-induced fractionation in surface agro-ecosystems, only biodegradation was included in the model. Since not significant alteration of the isotope composition of pollutants was expected during sorption and ageing (Schmidt et al., 2004; Droz et al., 2021), the ratios of light to heavy isotopologues did not significantly vary during sorption and ageing processes (Eq. 5, first term). In our case, since isotope fractionation associated with sorption and ageing processes is expected to be negligible, the observed isotope fractionation can be attributed primarily to biodegradation. This justifies the exclusion of non-destructive processes from the isotope mass balance and supports the use of the model to distinguish between destructive, i.e., biodegradation, and non-destructive processes, thereby enabling a quantitative evaluation of the contribution of biodegradation to pesticide dissipation. Altogether, representing pesticide mass (M) as separate light (l) and heavy (h) isotopologues, the change in aqueous and adsorbed phases is expressed as:

$$\frac{dM_{ads}}{dt} = -k_{age}\left(M_{ads}^l + M_{ads}^h\right) - k_{deg}\left(M_{ads}^l + \alpha M_{ads}^h\right) \tag{5}$$

$$\frac{dM_{aq}}{dt} = -k_{deg}\left(M_{aq}^l + \alpha M_{aq}^h\right) \tag{6}$$

where $k_{deg} = \ln(2) / DT_{50}$ and DT_{50} (days) was the observed degradation half-life in soil. Stable isotope fractionation associated with S-metolachlor degradation in soil was considered through the carbon fractionation factor (α_C), expressed as $\alpha_C = \varepsilon_C/1000$ + 1, where ε_C (‰) was the carbon stable isotope fractionation value of the targeted pesticide retrieved from a degradation reference experiment. Degradation rates for S-metolachlor freshly sorbed in the organic fraction of soil was assumed to be equal to degradation rates in the dissolved phase (Wu et al., 2011; Long et al., 2014). The reduction of bioavailability of the aged fraction of S-metolachlor as a function of the increasing fraction of irreversible sorbed S-metolachlor over time (Sander et al., 2006; Arias-Estevez et al., 2008; Torabi et al., 2020) was taken into account with the rate k_{irs} (d^{-1}) of irreversible sorption for the aged S-metolachlor mass (M_{age}, g):

$$\frac{dM_{age}}{dt} = -k_{irs}\left(M_{age}^l + M_{age}^h\right) \tag{7}$$

Decrease in M_{age} due to abiotic degradation (Xu et al., 2018) was not included, since it was unlikely to be significant under abiotic conditions in the studied aerobic soil (Torabi et al., 2020), even after 200 days of incubation (Alvarez-Zaldivar et al., 2018).

Pesticide degradation rates generally decline with soil depth due to reduced microbial activity (Cruz et al., 2008; Lutz et al., 2017) and increased sorption (Arias-Estevez et al., 2008) in deeper layer. However, the absence of concentration and CSIA data for S-metolachlor in subsoil prevented direct quantification of depth-dependence degradation. Following the approach used in advanced pesticide fate models such as MACRO (Garratt et al., 2003), the degradation rate (k_{deg}) in PiBEACH was modelled as a function of soil hydro-climatic conditions, such as soil temperature and water content. A dynamic degradation rate ($k_{Dynamic}$, d^{-1}) was calculated daily as a function of soil temperature (F_T; unitless) and of water content (F_θ ; unitless):

$$k_{Dynamic} = k_{Ref} \times F_T \times F_\theta \tag{8}$$

where k_{ref} (d^{-1}) was the degradation rate constant from degradation half-life (days) at reference conditions ($k_{Ref} = \ln(2) / DT_{50,Ref}$). A dynamic half-time $DT_{50,Dynamic}$ was derived to be compared to $DT_{50,Ref}$ ($DT_{50, Dynamic} = \ln(2) / k_{Dynamic}$).

For soil temperature dependence, the modified Arrhenius equation for low temperatures was considered (Boesten and Vanderlinden, 1991; Larsbo and Jarvis, 2003):

$$F_T = \begin{cases} 0, & if, T_C \le 0 \\ \frac{T_{K,Obs}-273.15}{5}\exp\left(\frac{E_a}{R}\left(\frac{1}{T_{K,Ref}} - \frac{1}{T_{K,Obs}}\right)\right), & if, 0 < T_C \le 5 \\ \exp\left(\frac{E_a}{R}\left(\frac{1}{T_{K,Ref}} - \frac{1}{T_{K,Obs}}\right)\right), & if\ T_C > 5 \end{cases} \tag{9}$$

where T_K and T_C were soil temperatures in Kelvin and Celsius, respectively and $T_{K,Ref}$ was the reference temperature at 293.15 K. E_a was the S-metolachlor activation energy (23.91 10^3 J mol^{-1}) (Jaikaew et al., 2017) and R was the gas constant (8.314 J mol^{-1} K^{-1}). This modified Arrhenius equation was validated against DT_{50} values derived from microcosm degradation experiments with S-metolachlor conducted at 20 and 30°C (Section 9 of SI, Figure S4).

Influence of water content followed Walker, (1974) and Larsbo and Jarvis (2003):

$$F_\theta = min\left(1.0, \left(\frac{\theta_t}{\theta_{Ref}}\right)^{\beta_\theta}\right) \quad\quad (10)$$

where β_θ was a calibration constant and θ_{Ref} the reference water content, which was set at 0.2 m^3 m^{-3}. Note that F_θ was slightly modified from Walker (1974), as microcosm experiments for S-metolachlor did not show an increase in degradation rates with increases in moisture contents (Figure S4).

Calibrating the PiBEACH parameters, as detailed in Section 2.6, was challenging and warranted the collection of an extensive dataset across the catchment throughout the growing season. This unique dataset incorporated isotopic signatures and comprised 103 topsoil samples analysed for S-metolachlor concentration and δ¹³C, 115 daily discharge measurements, and 51 river water samples at the outlet with corresponding S-metolachlor concentrations.

2.5 Model limitations

Although PiBEACH was primarily developed to simulate pesticides dissipation in topsoil, four aspects of its design may limit its application for predicting pesticide dynamics at the outlet of the headwater catchment. First, PiBEACH operates on a daily time step and is not suited to capture rapid flow dynamics, such as runoff generation and event-scale hydrological dynamics (Sheikh et al., 2009). Consequently, S-metolachlor concentrations and corresponding $\delta^{13}C$ values measured at the catchment outlet were not included in the model calibration objective function. This limitation could be addressed by coupling PiBEACH with a distributed event-based model, such as the Limburg Soil Erosion Model (OpenLISEM) (Baartman et al., 2012), which recently integrated a pesticide module (OLP) (Commelin et al., 2024). Second, PiBEACH uses a conceptual linear reservoir to represent shallow aquifer dynamics and does not explicitly simulate the effects of transit time distribution on pesticide release from groundwater to surface water (Hrachowitz et al., 2016). While incorporating transit time distribution into lumped reactive transport model has shown promise (Lutz et al., 2017), applying such approach in distributed model remains challenging, as demonstrated for nitrate (Kaandorp et al., 2021).

In addition, pesticide leaching across soil layers was considered without distinguishing matrix and preferential flows. Macropores can also play a significant role on pesticide breakthrough in the vadose zone (Urbina et al., 2020). However, the integration of macropores at the catchment scale necessitates advanced in situ measurements (Weiler, 2017), and a combination of geostatistical methods, pedotransfer functions or meta-models, i.e., simplified statistical models built with 1D soil reactive transport models such as MACRO (Lindahl et al. 2008).

PiBEACH integrates the main catchment compartments, including soil layers, vegetation and crops, and major processes controlling pesticide fate. However, plant uptake of S-metolachlor was not included, as it is likely negligible (Lefrancq et al., 2018). Additionally, pesticides wash off on plants was not considered in PiBEACH as S-metolachlor is a pre-emergent herbicide applied on bare soil.

Considering degradation in reactive transport models as a lumped process with only one half-life parameter is a strong simplification which may alter the predictability of degradation in models. However, this limitation is shared among existing pesticide transport models (Leistra et al., 2001; Lindahl et al, 2008; Lutz et al., 2017; Gatel et al.,2020). The implementation of soil temperature and moisture dependence for pesticide degradation, as proposed in this study, may strengthen the description of degradation within the catchment and across the hydrological or growing season (Gassmann 2021). Nonetheless, soil temperature and moisture are also forcing variables of the soil microbial activity, and thus of biodegradation, which remains extremely difficult to characterize and conceptualize with respect to pesticide transformation (Imfeld and Vuilleumier, 2012; Bongiorno, 2020; Höhener et al., 2022) for implementation in reactive models at the catchment scale.

2.6 Model uncertainty assessment

The GLUE and formal Bayesian methods are commonly used methods to quantify the uncertainty of hydrological models and provide distributions of parameters and water discharges. Bayesian methods are more convenient to calculate the uncertainty interval of one-step ahead forecasting with a formal or exact likelihood function (Jin et al., 2010). In contrast, the GLUE method integrates a true calibration process in which both inputs and model structural errors contribute to uncertainties of the model outputs (Beven et al., 2007). The GLUE method was thus adopted in our study to calibrate PiBEACH and retrieve output uncertainties. Rather than seeking an optimal model solution, the GLUE approach recognizes that more than one model structure or parameter set may lead to acceptable model results, i.e. equifinality (Beven and Binley, 1992). The GLUE method involved a sampling method of PiBEACH parameters values, an objective function incorporating observed dataset (i.e., topsoil S-metolachlor concentration only, then combined with S-metolachlor $\delta^{13}C$), a threshold of this objective function to select behavioural parameter sets, and the calculation of posterior probability distributions for parameters and uncertainties associated to the outputs of PiBEACH.

For the sampling method of parameters, PiBEACH required the calibration of 43 parameters (Table S3 in the Supplement). The range, i.e. min-max values, of these parameters were defined based either on literature or field data collected in 2012 and 2016 (Lefrancq et al., 2017 and 2018; Alvarez-Zaldivar et al., 2018). These parameters were assumed to be a priori uniformly distributed within these min and max values (Table S3 in the Supplement). To reduce the number of runs required by the GLUE method, three steps were successively applied. First, a pre-sensitivity global analysis based on the Morris method (Morris, 1991; Herman and Usher, 2017; Campolongo et al., 2007) was conducted with the SALib Python library for sensitivity analysis (section 10 of the Supplement) to select the most sensitive parameters. Although the Morris method yields a qualitative indication of relative parameter importance, it is efficient compared to other sensitivity approaches (Gan et al., 2014) that

screen for sensitive parameters (Herman et al., 2013). The mean and standard deviation of the elementary effects (EE) for each parameter were calculated as required by the Morris method. The mean represents the overall effect of a parameter on the model output, while the standard deviation captures the potential for interactions or non-linear effects. Parameters with a mean EE of zero or near zero, indicating negligible impact, were excluded, resulting in the removal of 21 parameters. The sensitivity analysis was conducted for the following outputs: S-metolachlor concentrations at the outlet; concentrations in composite topsoil transects (North, Valley, and South); discharge at the outlet; and isotope signatures both in the river at the outlet and within the topsoil composite transects. The EE statistics for the 25 retained parameters are shown in Figures S5 and S6 of the Supplement for each output variable.

The Morris method allowed to reduce the PiBEACH parameter number from 43 to 25 (Table S3 in the Supplement). Second, a Latin-Hypercube sampling (Herman and Usher, 2017) was used to reduce the numbers of runs (n = 2500) to cover the parameter space for the 25 parameters. To further reduce the computation time, the GLUE assessment focused on the growing period (March 19th to July 12th, 2016), where pesticide degradation and exports are of most significance. Initial hydrological state was estimated from a spin-up period of one full hydrological year (Oct. 1st, 2015 - Sept. 30th, 2016) and hydrological parameters calibrated against observed discharge at the catchment outlet (March 19th and July 12th, 2016) using particle swarm optimization (Bratton et al., 2007).

For the second step of the GLUE method, the Kling-Gupta Efficiency (KGE) (Gupta et al., 2009) metric was adopted as the objective function to maximize during calibration. Goodness of fit between simulations and observations are given relative to a maximum efficiency of 1 and given by:

$$KGE = 1 - \sqrt{(r-1)^2 + (\alpha_{KGE} - 1)^2 + (\beta_{KGE} - 1)^2} \qquad (11)$$

where r is the linear correlation coefficient between simulated and observed values, $\alpha_{KGE} = \sigma_i / \sigma_0$, and $\beta_{KGE} = \mu_i / \mu_0$, where σ and μ denoting the standard deviation and mean of simulated and observed values, respectively.

The KGE metric was selected to provide equal weight across correlation, bias and variability measures. The Kling–Gupta Efficiency (KGE) provides a more balanced assessment of model performance than traditional metrics such as the Mean Squared Error (MSE) or Nash–Sutcliffe Efficiency (NSE), which often favor parameter sets that underestimate output variability (Gupta et al., 2009). Three KGE metrics were calculated with (i) KGE_{SM} with weekly topsoil S-metolachlor concentration, (ii) KGE_{δ} with weekly topsoil $\delta^{13}C$ and (iii) KGE_Q with daily discharge at the outlet. The KGE metrics were successively built to assess the benefit of CSIA by incorporating topsoil S-metolachlor concentration only or in combination with topsoil S-metolachlor $\delta^{13}C$ observations. For the latter, KGE metric incorporates topsoil S-metolachlor concentration and $\delta^{13}C$ from (i) individual plot observations (13 black dots, Fig. 1), (ii) aggregated plot observation along three transects across

the catchment (North, Valley and South transect, Fig. 1) and (iii) transect composite soil (green dots, Fig. 1). These three approaches to aggregating topsoil data were developed to determine the minimum sampling effort for S-metolachlor concentration and $\delta^{13}C$ required to minimise uncertainties in PiBEACH model outputs.

According to the classification proposed by Kling et al. (2012) and subsequently adopted by Towner et al. (2019), the goodness-of-fit between simulated and observed variables is categorised as "very poor" for KGE $\leq$ 0, "poor" for KGE $\leq$ 0.5, "intermediate" for KGE $\leq$ 0.75, and "good" for KGE > 0.75, the threshold to retain acceptable model results runs (out of 2500 simulation runs) for topsoil S-metolachlor degradation and transport was set to KGE_{SM} >0.5 and KGE_{Q} >0.5. An additional and more stringent criterion (KGE_{δ} > 0.8) was applied to weekly topsoil $\delta^{13}C$ data to maximise its value as an indicator of degradation processes. These thresholds were ultimately selected as a compromise, enabling the retention of simulations with at least intermediate accuracy while preserving a sufficient number of parameter sets to support the derivation of outputs with robust confidence intervals.

In the final step of the GLUE procedure, the distributions of the 25 most sensitive parameters were extracted from the subset of acceptable parameter sets, i.e. KGE_{SM} >0.5 and KGE_{Q} >0.5 and KGE_{δ} >0.8. PiBEACH outputs were then expressed as the mean considering the 95 % confidence intervals based on these parameter sets, excluding the lower 2.5% and the upper 2.5% of acceptable simulations.

2.7 Metrics of pesticide persistence and transport risks

Six metrics were derived from PiBEACH outputs to assess S-metolachlor persistence and transport risk at the catchment scale. Expressed as percentages of the applied mass, these metrics included: (1) S-metolachlor degradation, (2) the remaining bioavailable mass of S-metolachlor (BAM) in the topsoil (i.e., dissolved and reversibly sorbed S-metolachlor), (3) S-metolachlor export to the catchment outlet via runoff and drainage, (4) off-site transport of S-metolachlor through leaching, (5) the remaining mass of irreversibly sorbed S-metolachlor (i.e., aged S-metolachlor), and (6) S-metolachlor volatilization, from the first application on March 19 (day 0) to July 12, 2016 (day 115). The first three metrics were also derived from field observations to evaluate the predictive accuracy of PiBEACH. Observed BAM in the topsoil was estimated through spatial extrapolation of weekly soil samples. The observed S-metolachlor degradation was estimated using the mean $\delta^{13}C$ derived from the same spatial extrapolation, combined with the enrichment factor (ε) obtained from microcosm lab-scale experiments using soil from Alteckendorf. Export to the outlet was calculated by integrating continuous discharge measurements with sub-weekly river S-metolachlor concentrations. The remaining three metrics, leaching, volatilization, and aging, could not be estimated from field data due to limitations of the catchment-scale sampling campaign and were therefore not computed from observations.

3 Results and discussion

3.1 Topsoil hydro-climatic dynamics and effect on S-metolachlor degradation rates

450

Simulated topsoil (z_0) water contents showed substantial variability, consistent with weekly field measurements (Fig. 3A) and previous application of the BEACH model in catchments with similar soils, crops and conditions (Sheikh et al., 2009). Simulated discharges at the catchment outlet showed reasonable agreement with observations (Fig. 3B), with a maximum KGE_Q of 0.75, demonstrating the model's ability to capture prevailing hydrological dynamics. However, PiBEACH slightly

455 overestimated runoff generation, a known limitation related to the underlying assumptions of the SCS-CN method (Section 6.2 in the Supplement), and the use of a daily time step, which does not resolve sub-daily rainfall intensity. Hydro-climatic variability drove changes in the simulated degradation rates ($k_{Dynamic}$) and associated half-times ($DT_{50,Dynamic}$) of S-metolachlor over time (Fig. 3C). Low S-metolachlor degradation rates during the first 10 days ($DT_{50} = 46 \pm 17$ d) coincided with cold (7.1 $\pm$ 1.7 °C) and dry period (7.4 mm of rainfall) (Fig. 3A). In contrast, increasing degradation rates ($DT_{50} = 22 \pm 2$ d) between 50

460 to 120 days following the first application of S-metolachlor were associated with warmer conditions (16.9 $\pm$ 3.6 T°C). Between March and July, topsoil temperatures increased, creating a stronger vertical temperature gradient and leading to reduced degradation activity at greater depths. In July, for instance, DT_{50} values were estimated at 25 days in the topsoil (Fig. 3C) and 34 days at 2 m depth (data not shown), consistent with predictions from the lumped model developed by Lutz et al. (2017) for this catchment. Simulated S-metolachlor concentrations (Fig. 3D) and carbon isotope ratios (Fig. 3E) in topsoil aligned with

465 weekly field observations, confirming the model's ability to reproduce both concentration dynamics and isotopic trends.
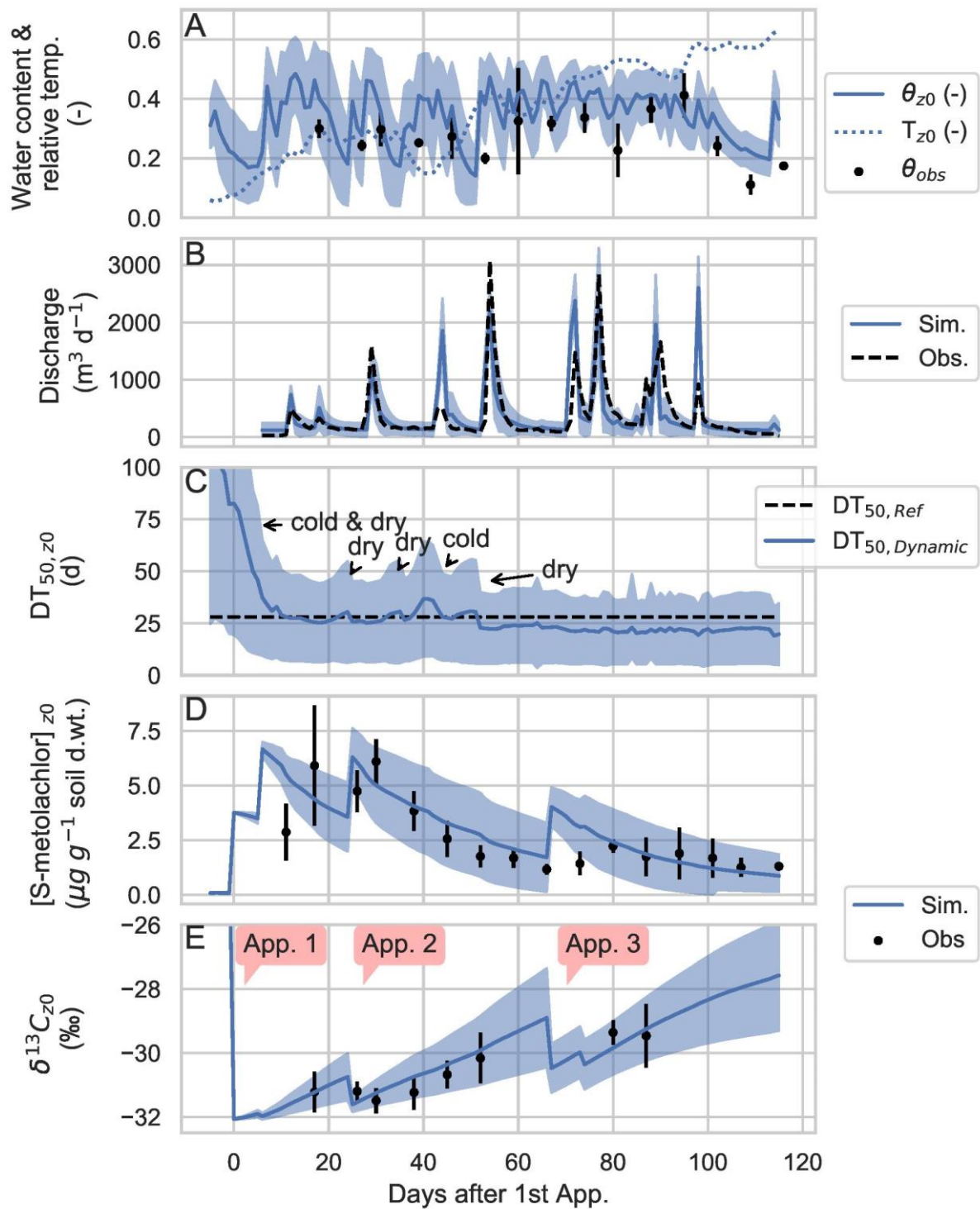
Figure 3: Predicted water content (m^3 m^{-3}) and relative topsoil temperatures ($T_{z0}/T_{air, max}$; with $T_{air, max}$ = 27°C) in the topsoil layer (z_0: 0-1cm) from March 14 (day -5, before first application) and July 12 (day 115). Shaded area indicates the 95 % confidence intervals (CI). Weekly observed water content (θ_{obs}) in topsoil is also shown (A), with error bars reflecting uncertainties in soil bulk density (used for gravimetric-to-volumetric conversion) and the standard error of gravimetric water content measurements. (B) Simulated and observed daily outlet discharge at the catchment scale, with the shaded area representing 95 % CI of the model ensemble. (C) Simulated mean dynamic degradation half-life ($DT_{50, Dynamic}$) of S-metolachlor in the topsoil (z_0), 95 % CI and the reference half-life ($DT_{50, Ref}$) shown for comparison. (D) Simulated and observed S-metolachlor concentrations composite topsoil transects (z_0), with error bars showing the standard deviation of measured values. (E) Simulated and observed $\delta^{13}C$ values of S-metolachlor in topsoil, with error bars showing the standard deviation. Application periods are marked as App. 1 (days 0 and 6), App. 2 (day 25), and App. 3 (days 67 and 74).

Out of 2500 simulation runs generated, 672 were deemed acceptable based on hydrological and concentration performance criteria (*KGE_Q* >0.5 and *KGE_{SM}* >0.5). Applying an additional constraint based on isotope data (*KGE_δ* >0.8) further reduced the ensemble of acceptable simulations to 244 simulations. Thus, only 36% of the acceptable runs also provided a reliable prediction of S-metolachlor degradation. In contrast, the remaining 64% accurately simulated hydrology and soil concentrations but showed poorer performance in reproducing degradation dynamics, as indicated by a wider range of $DT_{50,Ref}$ values (Fig. 4). These results highlighted the added value of including CSIA data during model calibration to constrain degradation parameters more effectively.

3.2 Uncertainty reduction through incorporation of CSIA data

This section underlines the benefit of incorporating topsoil CSIA data during model calibration (WIC: with isotope constraint) compared to no isotope constraint (NIC). For the composite transect soil (Fig. 4), the mean $DT_{50,Ref}$ values (μ; Eq. 8) were similar between NIC and WIC calibrations. However, the standard deviation of $DT_{50,Ref}$ was twice as large for NIC, indicating significantly higher uncertainty. This demonstrates that including CSIA data in the calibration phase substantially improved the constraint on S-metolachlor degradation estimates.
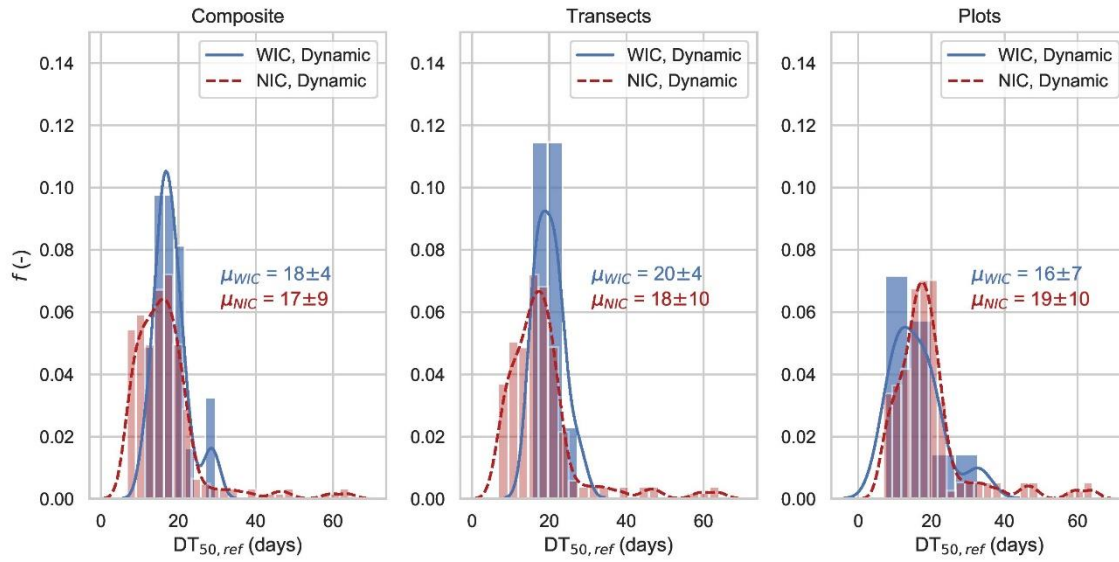
Figure 4: Distribution of calibrated DT_{50} values for 2,500 runs, shown for models without isotope constraints (NIC, $n = 672$) and with isotope constraints (WIC, $n = 244$), across three sampling resolutions: composite transect, transect and plot-scale soils. NIC simulations were selected based on $KGE_{SM} > 0.5$ and $KGE_Q > 0.5$, while WIC simulation also included $KGE_\delta > 0.8$. Mean $DT_{50,Ref}$ distributions are indicated by solid (WIC) and dotted (NIC) lines, and standard deviations are reported as $\mu \pm$ SD.

Reducing uncertainty in estimates of pesticide degradation in soil during the calibration of reactive transport models during calibration is crucial, as degradation half-lives can vary by one order of magnitude depending on the compound (Wang et al., 2018), largely affected by hydro-climatic and soil conditions. In this study, the WIC calibration yielded mean $DT_{50,Ref}$ below 20 days, with low standard deviations (SD <7 days; Fig. 4), indicating that aerobic degradation of S-metolachlor, typically reported between 14 and 21 days (Lewis et al., 2016), was the dominant process in Alteckendorf topsoil. In contrast, anaerobic degradation, characterized by longer half-lives ($DT_{50} = 23 - 62$ days; Seybold et al., 2001; Long et al., 2014), appeared to play a limited role.

The mean calibrated $DT_{50,Ref}$ values for transect composite soil, individual transects across the catchment, and plot resolutions differed by less than four days (Fig. 4). However, standard deviations reflecting uncertainty, were approximately 50% lower when isotopic constraints (WIC) were applied, compared to calibrations without isotopic constraints (NIC), for both transect composite and transect-scale data. At the plot scale, uncertainty remained unchanged. These results indicated that increasing resolution (plots > transects > transect composite samples) did not significantly improve model calibration in this catchment. Therefore, pooling transect samples into a single composite soil sample was sufficient for CSIA-based calibration, while also

reducing sampling and analytical efforts. This approach may reliably capture variations in pesticide degradation at the catchment scale.

Integration of CSIA data into PiBEACH yielded an isotope fractionation factor of εC = –2.7 ± 0.6 ‰ for S-metolachlor
515   degradation in topsoil, exceeding previously reported values (Alvarez-Zaldivar et al., 2018: –1.5 ± 0.5 ‰; Lutz et al., 2017: –
1.3 ± 0.5 ‰). This discrepancy likely reflects differences in environmental conditions, microbial activity, and transformation pathways, though it remains within the model ensemble's uncertainty range. Compared to laboratory-derived estimates, the stronger fractionation observed suggests either alternative degradation pathways or the influence of distinct microbial consortia at the catchment scale, relative to laboratory conditions. These findings underscore the importance of site-specific calibration
520   in CSIA applications and highlight the value of model ensemble approaches in capturing the range of degradation processes in heterogeneous agro-ecosystems. While previously reported εC values may slightly overestimate degradation in some field settings, the calibration of ensemble modelling with integrated CSIA data provides a more robust and field-relevant assessment of pesticide transformation. However, these findings necessitate further confirmation with a validation dataset, which was not available for the targeted catchment.

525   **3.3 Metrics of pesticide persistence and transport risks**

Six metrics were derived from calibrated PiBEACH outputs to evaluate S-metolachlor persistence in soil and its transport risk via leaching and runoff from topsoil across the catchment. Each metric was expressed as a percentage of applied S-metolachlor and included: (i) S-metolachlor degradation (Fig. 5A), (ii) remaining bioavailable mass of S-metolachlor (BAM) in topsoil (i.e. dissolved and reversibly-sorbed S-metolachlor; Fig. 5B), (iii) remaining mass of irreversibly sorbed S-metolachlor (aged;
530   Fig. 5E), (iv) off-site transport of S-metolachlor by leaching (Fig. 5D), (v) S-metolachlor volatilization (Fig. 5F), and (vi) S-metolachlor export to the catchment outlet by runoff and drainage (Fig. 5C). All metrics were calculated from the first application on March 19 (day 0) to July 12, 2016 (day 115). For two metrics, degradation and remaining mass in topsoil, PiBEACH closely matched observations (Fig. 5A, 5B and section 4 of the Supplement). The modelled degradation extent (72 ± 13%) was consistent with the value derived from $\delta^{13}C$ measurements on composite transect soil and the Rayleigh equation
535   (68 ± 1%) on day 87, corresponding to the last quantifiable soil isotope measurement (Fig. 5A). By day 115, the modelled degradation constituted the primary component of the mass balance, accounting for 82 ± 21% of the applied S-metolachlor mass. The remaining bioavailable mass (BAM) was estimated from measured concentrations and transect areas (Fig. 1, Fig. S1). The extrapolated remaining BAM from transect composite soil was 12 ± 8%, which fell within the modelled range at day 115 (18 ± 3%). The model slightly overestimated the export of S-metolachlor in river to the outlet (2 ± 6%) in comparison to
540   the observed values (0.5 ± 0.1%), which were not mobilised during calibration. However, this difference remains within the model's uncertainty range. It is important to note that observed exports were based solely on the dissolved phase, as particulate-bound S-metolachlor (> 0.7 µm) remained below quantification limits in all river water samples. The S-metolachlor export metric depends on PiBEACH ability to simulate daily discharge. Although PiBEACH was originally designed to initialize sub-

hourly, event-based distributed models like Openlisem-OLP (Commelin et al., 2024), it also demonstrated a reasonable ability to reproduce daily discharge dynamics (Fig. 3B), consistent with prior applications in similar catchments (Sheikh et al., 2009). Finally, S-metolachlor volatilisation predicted was below (<1 %) during the first 120 h after application, in line with the low vapor pressure of S-metolachlor (= 1.7 mPa, Lewis et al., 2016). However, volatilization rates ranging from 5 to 63 % of the applied mass has been reported under variable meteorological conditions (Gish et al., 2011).

550
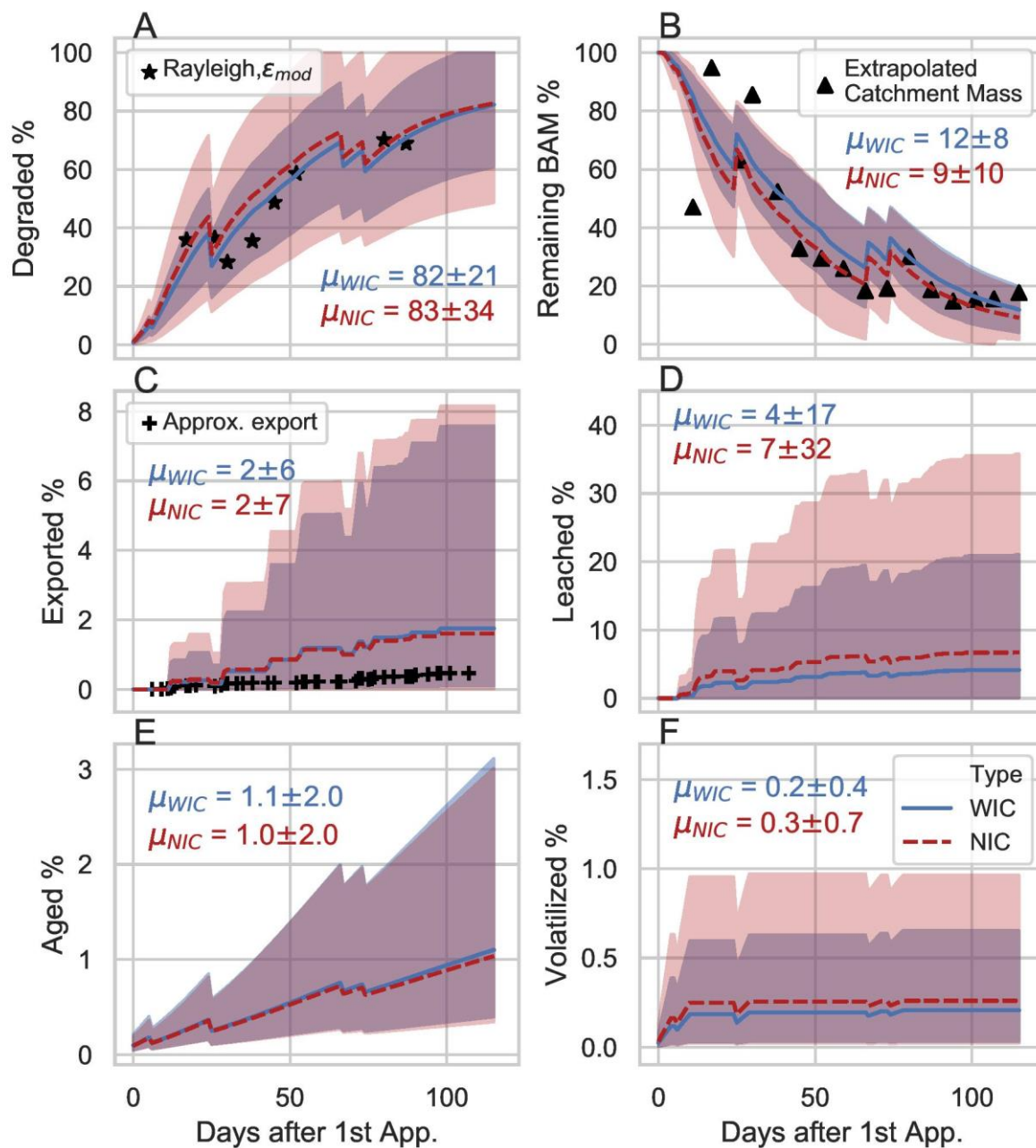
Figure 5: Pesticide dissipation processes and corresponding ensemble mean from a total of 672 simulations without isotope constraints (NIC, dotted line) and 244 simulations with isotope constraints (WIC, solid line). The 95% confidence intervals (CIs) are shown in red for NIC and blue for WIC. All metrics are expressed as percentages of the applied cumulative S-metolachlor mass across the catchment, starting

from the first application on March 19, 2016. Final dissipation values (μ_{WCI} and $\mu_{NIC} \pm 95$ % CI) are reported for day 115. Black markers indicate estimates derived from catchment-scale mass balances based on farmer surveys (Supplement, Sections S3 and S4).

560   The six pesticide transport metrics confirmed that incorporating CSIA data reduced the uncertainty of degradation estimates and other dissipation processes simulated by the PiBEACH model. Comparison of 95 % confidence intervals for showed that, by the end of the season (day 115), uncertainty was reduced by half in the WIC ensemble (with CSIA data) compared to the NIC ensemble (without CSIA data). Although the mean S-metolachlor degradation was similar for both dynamic DT_{50} models at the end of the season (i.e., $\Delta\mu = 1$ %), the uncertainty around degradation extent was 60% higher in the NIC ensemble. The

565   higher uncertainty propagated to other processes; for example, both mean and uncertainties of S-metolachlor leaching were twice as high in the NIC simulations compared to WIC. The wide 95% confidence intervals observed for the six metrics suggest that the thresholds used for the objective function, particularly $KGE_{SM} > 0.5$ and $KGE_Q > 0.5$, may need to be increased to reduce uncertainty. As previously noted in the application of the GLUE method (Jin et al., 2010), selecting an optimal threshold is inherently challenging, as it involves a trade-off between the computational effort required to retain a sufficient number of

570   acceptable simulations and the resulting width of the confidence intervals.

This modelling framework, applied to the same compound and catchment as in Lutz et al. (2017), provides insights into the benefits and limitations of using $\delta^{13}C$ data from soil and river samples to constrain reactive transport models. The lumped model by Lutz et al. (2017) focuses on $\delta^{13}C$ values at the catchment outlet, providing an integrated signature of degradation processes across the catchment. In contrast, PiBEACH allowed evaluation of the added value of topsoil $\delta^{13}C$ data for

575   constraining degradation kinetics. Model predictions for three components of the S-metolachlor mass balance, degraded mass, remaining mass in topsoil, and export at the outlet, were validated against observations. Due to limitations in representing rapid surface off-site transport associated with runoff and erosion, PiBEACH did not incorporate $\delta^{13}C$ data from river into the calibration. However, future coupling of PiBEACH with an event-based model like OpenLISEM-OLP could enable simultaneous integration of both topsoil and river $\delta^{13}C$ datasets, improving constraints on degradation and enhancing

580   simulation of fast-flow transport during high-intensity rainfall-runoff events.

In summary, $\delta^{13}C$ data from both soil and river samples can enhance model calibration by constraining degradation processes along different transport pathways. Lumped models (e.g., Lutz et al., 2017) and distributed models like PiBEACH each offer complementary perspectives on pesticide dynamics. However, only a distributed model can account for spatial heterogeneity across the catchment and support management decisions. PiBEACH also provides spatially explicit outputs on pesticide

585   concentrations, hydraulic properties, and topsoil moisture as critical inputs for initializing distributed event-based models. A large portion of the outlet data, i.e. discharge for calibration (as part of the KGE objective function), and discharge and S-metolachlor concentrations for evaluating export, was used to assess model performance. Nevertheless, due to limitations of PiBEACH's conceptual structure and daily resolution, the comparison between observed and simulated reactive transport was limited, unlike previous lumped approaches (Lutz et al., 2017). The forthcoming PiBEACH–OpenLISEM-OLP modelling

590 effort will explore the added value of incorporating observed S-metolachlor concentrations and isotopic signatures at the outlet into the calibration process.

This study demonstrates that even a moderate sampling effort, including weekly CSIA measurements from composite topsoil samples across the catchment, can effectively identify hot spots and hot moments of pesticide degradation at the catchment scale. In PiBEACH, degradation is primarily driven by soil temperature and moisture, which exhibits clear seasonal and

595 vertical gradients. As a result, degradation hotspots were consistently located in the topsoil. In contrast, soil moisture, although more spatial variable than temperature, played a secondary role. No significant spatial differences in DT_{50} were observed among plots treated with S-metolachlor over the growing season. The limited spatial variation in simulated DT_{50} across the catchment does not diminish the value of PiBEACH's distributed nature, particularly when considering its future integration with distributed event-based models such as OpenLISEM-OLP. This coupling remains essential for simulating surface

600 transport during rainfall events and refining predictions of pesticide fate under dynamic hydrological conditions.

As the field of pesticide CSIA evolves, through multi-element CSIA applications (Torrentó et al., 2021; Höhener et al., 2022) and the development of passive sampling techniques (Gilevska et al., 2022a), the ability to evaluate dissipation processes and distinguish between competing pathways (Elsner and Imfeld, 2016; Hofstetter et al., 2024) will enhance assessments of pesticide degradation in agricultural soils and enable more robust catchment-scale modelling.

605 **3 Conclusion**

This study addresses the gap between the increasing complexity of reactive transport models and the limited availability of field data for their calibration. Although the representation of interactions between hydro-climatic conditions, biogeochemical processes, and degradation dynamics has improved significantly in recent decades, it remains oversimplified in many 2D catchment models (Lutz et al., 2013) or is not explicitly defined (DeMars et al., 2018). Incorporating more detailed physical

610 and biological representations of degradation catchments increases model complexity and uncertainty, making it essential to acquire additional data to constrain parameter ranges and reduce equifinality. Our findings suggest that using only topsoil pesticide concentrations and discharge measurements is insufficient to effectively constrain reactive transport models at the catchment scale. We demonstrated that incorporating complementary data, such as pesticide CSIA data (Fenner et al., 2013, Elsner and Imfeld, 2016; Hofstetter et al., 2024), can help differentiate between degradative and non-degradative processes

615 contributing to observed concentration declines. In many cases, carbon isotope data ($\delta^{13}C$) alone may be adequate to provide evidence of in situ degradation, thereby supporting pesticide mass balance closure and improving model calibration at the catchment scale. The next step should involve confirming these findings with a validation dataset, which was not available for the targeted catchment. Looking ahead, multi-element CSIA has the potential to further elucidate competing degradation

pathways (Höhener et al., 2022). To improve model accuracy, future research should also consider the dynamics of microbial functional diversity, biomass, and biodegradation potential (Konig et al., 2018).

Our results highlight the potential of topsoil CSIA data to inform pesticide management strategies by providing more reliable estimates of degradation and transport processes at the headwater catchment scale. Given the strong effect of hydro-climatic factors on pesticide degradation and transport, especially under changing rainfall and temperature regimes driven by climate change (Barrios et al., 2020), it is essential to account for these dynamics is pesticide fate assessments. Furthermore, risk metrics for pesticide risk assessment often require probabilistic approaches, including confidence intervals (Lutz et al., 2013). Therefore, to support decision-making and ecotoxicological assessments, hydrological models should systematically incorporate uncertainty frameworks to capture the full range of parameter values affecting pesticide transfer risks.

4 Code availability

The codes developed for this study are available from the corresponding author upon request.

5 Data availability

The data produced for this study are available from the corresponding author upon request.

6 Author contributions

PAZ performed conceptualization, data curation, formal analysis, investigation and writing. PVD developed the agronomical module, produced associated results, and performed writing. SP and GI performed conceptualization, funding acquisition, project administration, supervision and writing – review & editing.

7 Supplement

The supplement related to this article includes a summary of hydro-climatic conditions, detailed catchment and sampling descriptions, farmer survey results, $\delta^{13}C$ analysis and detailed model descriptions and is available in assets section.

8 Competing interests

The authors declare that they have no conflict of interest.

9 Acknowledgements

P. Alvarez-Zaldivar was supported by an Initiatives d'excellence (IDEX) fellowship of the Strasbourg University. This work is funded by the French National research Agency ANR through grant ANR-18-CE04-0004-01, project DECISIVE. The authors thank S. Wisselmann, M. Levasseur, C. Wiegert, and B. Guyot for support in sampling and analysis and R. Coupe for helpful comments on the article's structure and organization. We would also like to thank the Alteckendorf farmers for their collaboration during the field study.

10 References

Ahuja, L. and Lehman, O.: The extent and nature of rainfall-soil interaction in the release of soluble chemicals to runoff, J. Environ. Qual., 12, 34–40, https://doi.org/10.2134/jeq1983.00472425001200010005x, 1983.

Alvarez-Zaldivar, P., Centler, F., Maier, U., Thullner, M., and Imfeld, G.: Biogeochemical modelling of in situ biodegradation and stable isotope fractionation of intermediate chloroethenes in a horizontal subsurface flow wetland, Ecol. Eng., 90, 170–179, https://doi.org/10.1016/j.ecoleng.2016.01.0370, 2016.

Alvarez-Zaldivar, P., Payraudeau, S., Meite, F., Masbou, J., and Imfeld, G.: Pesticide degradation and export losses at the catchment scale: Insights from compound-specific isotope analysis (CSIA), Water Res., 139, 198–207, https://doi.org/10.1016/j.watres.2018.03.061, 2018.

Ammann, L., Doppler, T., Stamm, C., Reichert, P., and Fenicia, F.: Characterizing fast herbicide transport in a small agricultural catchment with conceptual models, J. Hydrol., 586, https://doi.org/10.1016/j.jhydrol.2020.124812, 2020.

Antelmi, M., Mazzon, P., Hohener, P., Marchesi, M., and Alberti, L.: Evaluation of MNA in A Chlorinated Solvents-Contaminated Aquifer Using Reactive Transport Modeling Coupled with Isotopic Fractionation Analysis, Water, 13, 2945, https://doi.org/10.3390/w13212945, 2021.

Arias-Estevez, M., Lopez-Periago, E., Martinez-Carballo, E., Simal-Gandara, J., Mejuto, J., and Garcia-Rio, L.: The mobility and degradation of pesticides in soils and the pollution of groundwater resources, Agr. Ecosyst. Environ., 123, 247–260, https://doi.org/10.1016/j.agee.2007.07.011, 2008.

Baartman, J., Jetten, V., Ritsema, C., and de Vente, J.: Exploring effects of rainfall intensity and duration on soil erosion at the catchment scale using openLISEM: Prado catchment, SE Spain, Hydro. Process., 26, 1034–1049, https://doi.org/10.1002/hyp.8196, 2012.

Barrios, R., Akbariyeh, S., Liu, C., Gani, K., Kovalchuk, M., Li, X., Li, Y., Snow, D., Tang, Z., Gates, J., and Bartelt-Hunt, S.: Climate change impacts the subsurface transport of atrazine and estrone originating from agricultural production activities, Environ. Pollut., 265, https://doi.org/10.1016/j.envpol.2020.115024, 2020.

Beven, K. and Binley, A.: The future of distributed models - model calibration and uncertainty prediction, Hydro. Process., 6, 279–298, https://doi.org/10.1002/hyp.3360060305, 1992.

Beven, K., Smith, P., and Freer, J.: Comment on "Hydrological forecasting uncertainty assessment: incoherence of the GLUE methodology" by Pietro Mantovan and Ezio Todini, J. Hydrol., 338, 315–318, https://doi.org/10.1016/j.jhydrol.2007.02.023, 2007.

Blázquez-Pallí, N., Shouakar-Stash, O., Palau, J., Trueba-Santiso, A., Varias, J., Bosch, M., Soler, A., Vicent T., Marco-Urrea, E., and Rosell, M.: Use of dual element isotope analysis and microcosm studies to determine the origin and potential anaerobic biodegradation of dichloromethane in two multi-contaminated aquifers, Sci. Total Envir., 696, 134066, DOI10.1016/j.scitotenv.2019.134066, 2019.

680   Boesten, J. and Vanderlinden, A.: Modeling the influence of sortpion and transformation on pesticide leaching and persitence, J. Environ. Qual., 20, 425–435, https://doi.org/10.2134/jeq1991.00472425002000020015x, 1991.

Bongiorno, G.: Novel soil quality indicators for the evaluation of agricultural management practices: a biological perspective, Front Agric Sci Eng, 7, 257, https://doi.org/10.15302/J-FASE-2020323, 2020.

Bratton, D., and Kennedy, J.: Defining a standard for particle swarm optimization, 2007 IEEE SWARM Intelligence 685   Symposium, 120-+, https://doi.org/10.1109/SIS.2007.368035, 2007.

Broers, H.P., van Vliet, M., Kivits, T., Vernes, R., Brussée, T., Sültenfuß, J., and Fraters, D.: Nitrate trend reversal in Dutch dual-permeability chalk springs, evaluated by tritium-based groundwater travel time distributions, Sci Total Environ., 15;951:175250. https://doi.org/10.1016/j.scitotenv.2024.175250, 2024.

Campolongo, F. Cariboni, J. Saltelli, A.: An effective screening design for sensitivity analysis of large models, Environ. Model. 690   Softw., 22 (10), 1509–1518, https://doi.org/10.1016/j.envsoft.2006.10.004, 2007.

Commelin, M.C., Baartman, J., Wesseling, J.G. and Jetten, V.: Simulating Event-Based Pesticide Transport with Runoff and Erosion; Openlisem-Pesticide V.1. Environ. Model. Softw., 174, 105960, https://doi.org/10.1016/j.envsoft.2024.105960, 2024.

Cruz, M., Jones, J., and Bending, G.: Study of the spatial variation of the biodegradation rate of the herbicide bentazone with 695   soil depth using contrasting incubation methods, Chemosphere, 73, 1211–1215, https://doi.org/10.1016/j.chemosphere.2008.07.044, 2008.

De Schepper, G., Therrien, R., Refsgaard, J., and Hansen, A.: Simulating coupled surface and subsurface water flow in a tile-drained agricultural catchment, J. Hydrol., 521, 374–388, https://doi.org/10.1016/j.jhydrol.2014.12.035, 2015.

DeMars, C., Zhan, Y., Chen, H., Heilman, P., Zhang, X., and Zhang, M.: Integrating GLEAMS sedimentation into RZWQM 700   for pesticide sorbed sediment runoff modeling, Environ. Modell. Softw., 109, 390–401, https://doi.org/10.1016/j.envsoft.2018.08.016, 2018.

Droz, B., Drouin, G., Maurer, L., Villette, C., Payraudeau, S., and Imfeld, G.: Phase Transfer and Biodegradation of Pesticides in Water-Sediment Systems Explored by Compound-Specific Isotope Analysis and Conceptual Modeling, Environ. Sci. Technol., 55, 4720–4728, https://doi.org/10.1021/acs.est.0c06283, 2021.

705   Dubus, I., Beulke, S., and Brown, C.: Calibration of pesticide leaching models: critical review and guidance for reporting, Pest Manag. Sci., 58, 745–758, https://doi.org/10.1002/ps.526, 2002.

Dubus, I., Brown, C., and Beulke, S.: Sensitivity analyses for four pesticide leaching models, Pest Manag. Sci., 59, 962–982, https://doi.org/10.1002/ps.723, 2003.

Eckert, D., Qiu, S., Elsner, M., Cirpka O.A.: Model complexity needed for quantitative analysis of high resolution isotope and 710   concentration data from a toluene-pulse experiment. Environ Sci Technol., 2, 47 (13), 6900-7. https://doi.org/10.1021/es304879d, 2013.

Elsner, M.: Stable isotope fractionation to investigate natural transformation mechanisms of organic contaminants: principles, prospects and limitations, J. Environ. Monitor., 12, 2005–2031, https://doi.org/10.1039/c0em00277a, 2010.

715 Elsner, M. and Imfeld, G.: Compound-specific isotope analysis (CSIA) of micropollutants in the environment - current developments and future challenges, Curr. Opin. Biotechnol., 41, 60–72, https://doi.org/10.1016/j.copbio.2016.04.014, 2016.

Fatichi, S., Vivoni, E., Ogden, F., Ivanov, V., Mirus, B., Gochis, D., Downer, C., Camporese, M., Davison, J., Ebel, B., Jones, N., Kim, J., Mascaro, G., Niswonger, R., Restrepo, P., Rigon, R., Shen, C., Sulis, M., and Tarboton, D.: An overview of current applications, challenges, and future trends in distributed process-based models in hydrology, J. Hydrol., 537, 45–60, https://doi.org/10.1016/j.jhydrol.2016.03.026, 2016.

720 Feigenbrugel, V., Le Calve, S., and Mirabel, P.: Temperature dependence of Henry's law constants of metolachlor and diazinon, Chemosphere, 57, 319–327, https://doi.org/10.1016/j.chemosphere.2004.05.013, 2004.

Fenner, K., Canonica, S., Wackett, L., and Elsner, M.: Evaluating Pesticide Degradation in the Environment: Blind Spots and Emerging Opportunities, Science, 341, 752–758, https://doi.org/10.1126/science.1236281, 2013.

Gan, Y., Duan, Q., Gong, W., Tong, C., Sun, Y., Chu, W., Ye, A., Miao, C., and Di, Z.: A comprehensive evaluation of various 725 sensitivity analysis methods: A case study with a hydrological model, Environ. Modell. Softw., 51, 269–285, https://doi.org/10.1016/j.envsoft.2013.09.031, 2014.

Garratt, J., Capri, E., Trevisan, M., Errera, G., and Wilkins, R.: Parameterisation, evaluation and comparison of pesticide leaching models to data from a Bologna field site, Italy, Pest Manag. Sci., 59, 3–20, https://doi.org/10.1002/ps.596, 2003.

Gassmann, M.: Modelling the Fate of Pesticide Transformation Products From Plot to Catchment Scale-State of Knowledge 730 and Future Challenges, Front. Environ. Sci., 9, 717738, https://doi.org/10.3389/fenvs.2021.717738, 2021.

Gatel, L., Lauvernet, C., Carluer, N., Weill, S., and Paniconi, C.: Sobol Global Sensitivity Analysis of a Coupled Surface/Subsurface Water Flow and Reactive Solute Transfer Model on a Real Hillslope, Water, 12, https://doi.org/10.3390/w12010121, 2020.

Gilevska, T., Masbou, J., Baumlin, B., Chaumet, B., Chaumont, C., Payraudeau, S., Tournebize, J., Probst, A., Probst, J.L., 735 Imfeld G.: Do pesticides degrade in surface water receiving runoff from agricultural catchments ? Combining passive samplers (POCIS) and compound-specific isotope analysis. Sci. Total Environ., 842, 156735, https://doi.org/10.1016/j.scitotenv.2022.156735, 2022a

Gilevska, T., Wiegert, C., Droz, B., Junginger, T., Prieto-Espinoza, M., Borreca, A., and Imfeld, G.: Simple extraction methods for pesticide compound-specific isotope analysis from environmental samples, METHODSX, 9, 740 https://doi.org/10.1016/j.mex.2022.101880, 2022b.

Gish, T., Prueger, J., Daughtry, C., Kustas, W., McKee, L., Russ, A., and Hatfield, J.: Comparison of Field-scale Herbicide Runoff and Volatilization Losses: An Eight-Year Field Investigation, J. Environ. Qual., 40, 1432–1442, https://doi.org/10.2134/jeq2010.0092, 2011.

Grundmann, S., Fuss, R., Schmid, M., Laschinger, M., Ruth, B., Schulin, R., Munch, J. C., and Schroll, R.: Application of 745 microbial hot spots enhances pesticide degradation in soils, Chemosphere, 68, 511–517, https://doi.org/10.1016/j.chemosphere.2006.12.065, 2007.

Gupta, H., Kling, H., Yilmaz, K., and Martinez, G.: Decomposition of the mean squared error and NSE performance criteria: Implications for improving hydrological modelling, J. Hydrol., 377, 80–91, https://doi.org/10.1016/j.jhydrol.2009.08.003, 2009.

750 Herman, J. and Usher, W.: SALib: An open-source Python library for Sensitivity Analysis, J. Open Source Softw., 2, 97, https://doi.org/10.21105/joss.00097, 2017.

Herman, J., Kollat, J., Reed, P., and Wagener, T.: Technical Note: Method of Morris effectively reduces the computational demands of global sensitivity analysis for distributed watershed models, Hydrol. Earth Syst. Sci., 17, 2893–2903, https://doi.org/10.5194/hess-17-2893-2013, 2013.

755 Hofstetter, T.B., Bakkour, R., Buchner, D., Eisenmann, H., Fischer, A., Gehre, M., Haderlein, S.B., Höhener, P., Hunkeler, D., Imfeld, G., Jochmann, M.A., Kümmel, S., Martin, P.R., Pati, S.G., Schmidt, T.C., Vogt, C., Elsner M.: Perspectives of compound-specific isotope analysis of organic contaminants for assessing environmental fate and managing chemical pollution. Nat Water 2, 14–30, https://doi.org/10.1038/s44221-023-00176-4, 2024.

Höhener, P., Guers, D., Malleret, L., Boukaroum, O., Martin-Laurent, F., Masbou, J., Payraudeau, S., and Imfeld, G.: Multi-
760 elemental compound-specific isotope analysis of pesticides for source identification and monitoring of degradation in soil: a review, Environ. Chem. Lett., https://doi.org/10.1007/s10311-022-01489-8, 2022.

Honti, M. and Fenner, K.: Deriving Persistence Indicators from Regulatory Water-Sediment Studies - Opportunities and Limitations in OECD 308 Data, Environ. Sci. Technol., 49, 5879–5886, https://doi.org/10.1021/acs.est.5b00788, 2015.

Hrachowitz, M., Benettin, P., van Breukelen, B., Fovet, O., Howden, N., Ruiz, L., van der Velde, Y., and Wade, A.: Transit
765 timesthe link between hydrology and water quality at the catchment scale, Wiley Interdisciplinary Reviews-Water, 3, 629–657, https://doi.org/10.1002/wat2.1155, 2016.

Hunkeler, D., Meckenstock, R. U., Sherwood Lollar, B., Schmidt, T. C., Wilson, J. T., Schmidt, T., and Wilson, J.: A guide for assessing biodegradation and source identification of organic ground water contaminants using compound specific isotope analysis (CSIA), US EPA, Ada, 2008.

770 Imfeld, G. and Vuilleumier, S.: Measuring the effects of pesticides on bacterial communities in soil: A critical review, Eur. J. Soil Biol., 49, 22–30, https://doi.org/10.1016/j.ejsobi.2011.11.010, 2012.

Jaikaew, P., Malhat, F., Boulange, J., and Watanabe, H.: Aspect of the degradation and adsorption kinetics of atrazine and metolachlor in andisol soil, Hell. Plant Prot. J., 10, 1–14, https://doi.org/10.1515/hppj-2017-0001, 2017.

Jin, X., Xu, C., Zhang, Q., and Singh, V.: Parameter and modeling uncertainty simulated by GLUE and a formal Bayesian
775 method for a conceptual hydrological model, J. Hydrol., 383, 147–155, https://doi.org/10.1016/j.jhydrol.2009.12.028, 2010.

Kaandorp, V., Broers, H., van der Velde, Y., Rozemeijer, J., and de Louw, P.: Time lags of nitrate, chloride, and tritium in streams assessed by dynamic groundwater flow tracking in a lowland landscape, Hydrol. Earth Syst. Sci., 25, 3691–3711, https://doi.org/10.5194/hess-25-3691-2021, 2021.

Kling, H., Fuchs, M., and Paulin, M.: Runoff conditions in the upper Danube basin under an ensemble of climate change
780 scenarios, J. Hydrol., 424, 264–277, https://doi.org/10.1016/j.jhydrol.2012.01.011, 2012.

Köhne, J., Köhne, S., and Simunek, J.: A review of model applications for structured soils: b) Pesticide transport, J. Contam. Hydrol., 104, 36–60, https://doi.org/10.1016/j.jconhyd.2008.10.003, 2009.

Konig, S., Worrich, A., Banitz, T., Harms, H., Kastner, M., Miltner, A., Wick, L., Frank, K., Thullner, M., and Centler, F.: Functional Resistance to Recurrent Spatially Heterogeneous Disturbances Is Facilitated by Increased Activity of Surviving Bacteria in a Virtual Ecosystem, Front. Microbiol., 9, https://doi.org/10.3389/fmicb.2018.00734, 2018.

Kopinke, F.D., Georgi, A., Imfeld, G., Richnow, H.H.,: Isotope fractionation of benzene during partitioning - Revisited. Chemosphere 168, 508-513, https://doi.org/10.1016/j.chemosphere.2016.11.029, 2017.

Lange, J., Olsson, O., Sweeney, B., Herbstritt, B., Reich, M., Alvarez-Zaldivar, P., Payraudeau, S., and Imfeld, G.: Fluorescent tracers to evaluate pesticide dissipation and transformation in agricultural soils, Sci. Total Environ., 619, 1682–1689, https://doi.org/10.1016/j.scitotenv.2017.10.132, 2018.

Larsbo, M. and Jarvis, N.: MACRO 5.0. A model of water and solute transport in macroporous soil. Technical description. Emergo 2033.6 Swedish University of Agricultural Sciences, Department of Soil Sciences, Uppsala, Sweden, 2003.

Larsbo, M. and Jarvis, N.: Simulating solute transport in a structured field soil: Uncertainty in parameter identification and predictions, J. Environ. Qual., 34, 621–634, https://doi.org/10.2134/jeq2005.0621, 2005.

Lefrancq, M., Van Dijk, P., Jetten, V., Schwob, M., and Payraudeau, S.: Improving runoff prediction using agronomical information in a cropped, loess covered catchment, Hydro. Process., 31, 1408–1423, https://doi.org/10.1002/hyp.11115, 2017.

Lefrancq, M., Payraudeau, S., Guyot, B., Millet, M., and Imfeld, G.: Degradation and Transport of the Chiral Herbicide S-Metolachlor at the Catchment Scale: Combining Observation Scales and Analytical Approaches (vol 51, pg 13231, 2017), Environ. Sci. Technol., 52, 5517–5517, https://doi.org/10.1021/acs.est.8b01118, 2018.

Leistra, M., van der Linden, A. M. A., Boesten, J. J. T. I., Tiktak, A., and van der Berg, F.: PEARL model for pesticide behaviour and emissions in soil-plant systems; Description of the processes in FOCUS PEARL v 1.1.1., 2001.

Lewis, K., Tzilivakis, J., Warner, D., and Green, A.: An international database for pesticide risk assessments and management, Hum. Ecol. Risk Assess., 22, 1050–1064, https://doi.org/10.1080/10807039.2015.1133242, 2016.

Long, Y., Li, R., and Wu, X.: Degradation of S-metolachlor in soil as affected by environmental factors, J. Soil Sci. Plant Nut., 14, 189–198, http://dx.doi.org/10.4067/S0718-95162014005000015, 2014.

Lutz, S. R., van Meerveld, H. J., Waterloo, M. J., Broers, H. P., and van Breukelen, B. M.: A model-based assessment of the potential use of compound-specific stable isotope analysis in river monitoring of diffuse pesticide pollution, Hydrol. Earth Syst. Sci., 17, 4505–4524, https://doi.org/10.5194/hess-17-4505-2013, 2013.

Lutz, S. R., van der Velde, Y., Elsayed, O. F., Imfeld, G., Lefrancq, M., Payraudeau, S., and van Breukelen, B. M.: Pesticide fate on catchment scale: conceptual modelling of stream CSIA data, Hydrol. Earth Syst. Sci., 21, 5243–5261, https://doi.org/10.5194/hess-21-5243-2017, 2017.

Malone, R., Ahuja, L., Ma, L., Wauchope, R., Ma, Q., and Rojas, K.: Application of the Root Zone Water Quality Model (RZWQM) to pesticide fate and transport: an overview, Pest Manag. Sci., 60, 205–221, https://doi.org/10.1002/ps.789, 2004.

Manfreda, S., Fiorentino, M., and Iacobellis, V.: DREAM: a Distributed model for Runoff, Evapotranspiration, and Antecedent Soil Moisture Simulation, Adv. Geosci, 2, 31–39, https://doi.org/10.5194/adgeo-2-31-2005, 2005.

Masbou, J., Höhener, P., Payraudeau, S., Martin-Laurent, F., Imfeld, G.: Stable isotope composition of pesticides in commercial formulations: The ISOTOPEST database. Chemosphere, 352 141488, https://doi.org/10.1016/j.chemosphere.2024.141488, 2024.

McGrath, G., Hinz, C., and Sivapalan, M.: Modeling the effect of rainfall intermittency on the variability of solute persistence at the soil surface, Water Resour. Res., 44, https://doi.org/10.1029/2007WR006652, 2008.

Medici, C., Wade, A., and Frances, F.: Does increased hydrochemical model complexity decrease robustness?, J. Hydrol., 440, 1–13, https://doi.org/10.1016/j.jhydrol.2012.02.047, 2012.

Molénat, J., Gascuel-Odoux, C., Davy, P., Durand P.: How to model shallow water-table depth variations: the case of the Kervidy-Naizin catchment, France, Hydrol. Process., 19, 901-920, https://doi.org/10.1002/hyp.5546, 2005.

Morris, M. D.: Factorial sampling plans for preliminary computational experiments, Technometrics, 33, 161–174, https://doi.org/10.2307/1269043, 1991.

Neitsch, S. L., Arnold, J. G., Kiniry, J. R., and Williams, J. R.: Soil and Water Assessment Tool. Theoretical Documentation. Version 2009.Texas Water Resources Institute Technical Report No. 406 Texas A&M University System College Station, Texas, USA. 647 pages, 2011.

Prieto-Espinoza, M., Weill, S., Belfort, B., Muller, E., Masbou, J., Lehmann, F., Vuilleumier, S., and Imfeld, G.: Water table fluctuations affect dichloromethane biodegradation in lab-scale aquifers contaminated with organohalides, Water Res., 203, https://doi.org/10.1016/j.watres.2021.117530, 2021.

Prueger, J., Gish, T., McConnell, L., McKee, L., Hatfield, J., and Kustas, W.: Solar radiation, relative humidity, and soil water effects on metolachlor volatilization, Environ. Sci. Technol., 39, 5219–5226, https://doi.org/10.1021/es048341q, 2005.

Sander, M., Lu, Y., and Pignatello, J.: Conditioning-annealing studies of natural organic matter solids linking irreversible sorption to irreversible structural expansion, Environ. Sci. Technol., 40, 170–178, https://doi.org/10.1021/es0506253, 2006.

Schmidt, T., Zwank, L., Elsner, M., Berg, M., Meckenstock, R., and Haderlein, S.: Compound-specific stable isotope analysis of organic contaminants in natural environments: a critical review of the state of the art, prospects, and future challenges, Anal. Bioanal. Chem., 378, 283–300, https://doi.org/10.1007/s00216-003-2350-y, 2004.

Schroll, R., Becher, H., Dorfler, U., Gayler, S., Hartmann, H., and Ruoss, J.: Quantifying the effect of soil moisture on the aerobic microbial mineralization of selected pesticides in different soils, Environ. Sci. Technol., 40, 3305–3312, https://doi.org/10.1021/es052205j, 2006.

Schwarzenbach, R. P.: Environmental organic chemistry, 2nd ed., Wiley, 2003.

Seybold, C., Mersie, W., and McNamee, C.: Anaerobic degradation of atrazine and metolachlor and metabolite formation in wetland soil and water microcosms, J. Environ. Qual., 30, 1271–1277, https://doi.org/10.2134/jeq2001.3041271x, 2001.

Sheikh, V., Visser, S., and Stroosnijder, L.: A simple model to predict soil moisture: Bridging Event and Continuous Hydrological (BEACH) modelling, Environ. Modell. Softw., 24, 542–556, https://doi.org/10.1016/j.envsoft.2008.10.005, 2009.

Sidoli, P., Lassabatere, L., Angulo-Jaramillo, R., and Baran, N.: Experimental and modeling of the unsaturated transports of S-metolachlor and its metabolites in glaciofluvial vadose zone solids, J. Contam. Hydrol., 190, 1–14, https://doi.org/10.1016/j.jconhyd.2016.04.001, 2016.

Steffens, K., Jarvis, N., Lewan, E., Lindstrom, B., Kreuger, J., Kjellstrom, E., and Moeys, J.: Direct and indirect effects of climate change on herbicide leaching - A regional scale assessment in Sweden, Sci. Total Environ., 514, 239–249, https://doi.org/10.1016/j.scitotenv.2014.12.049, 2015.

Stone, W., Gilliom, R., and Ryberg, K.: Pesticides in U.S. Streams and Rivers: Occurrence and Trends during 1992-2011, Environ. Sci. Technol., 48, 11025–11030, https://doi.org/10.1021/es5025367, 2014.

Thouement, H. A. A., Kuder, T., Heimovaara, T. J., and van Breukelen, B. M.: Do CSIA data from aquifers inform on natural degradation of chlorinated ethenes in aquitards?, J. Contam. Hydrol., 226, 103520, https://doi.org/10.1016/j.jconhyd.2019.103520, 2019.

Thullner, M., Fischer, A., Richnow, H., and Wick, L.: Influence of mass transfer on stable isotope fractionation, Appl. Microbiol. Biotechnol., 97, 441–452, https://doi.org/10.1007/s00253-012-4537-7, 2013.

Torabi, E., Wiegert, C., Guyot, B., Vuilleumier, S., and Imfeld, G.: Dissipation of S-metolachlor and butachlor in agricultural soils and responses of bacterial communities: Insights from compound-specific isotope and biomolecular analyses, J. Environ. Sci., 92, 163–175, https://doi.org/10.1016/j.jes.2020.02.009, 2020.

Torrentó, C., Ponsin, V., Lihl, C., Hofstetter, T. B., Baran, N., Elsner, M., and Hunkeler, D.: Triple-Element Compound-Specific Stable Isotope Analysis (3D-CSIA): Added Value of Cl Isotope Ratios to Assess Herbicide Degradation, Environ. Sci. Technol., 55, 13891–13901, https://doi.org/10.1021/acs.est.1c03981, 2021.

Towner, J., Cloke, H. L., Zsoter, E., Flamig, Z., Hoch, J. M., Bazo, J., Coughlan de Perez, E., and Stephens, E. M.: Assessing the performance of global hydrological models for capturing peak river flows in the Amazon basin, Hydrol. Earth Syst. Sci., 23, 3057–3080, https://doi.org/10.5194/hess-23-3057-2019, 2019.

Urbina, C., van den Berg, F., van Dam, J., Tang, D., and Ritsema, C.: Parameter sensitivity of SWAP-PEARL models for pesticide leaching in macroporous soils, Vadose Zone J., 19, https://doi.org/10.1002/vzj2.20075, 2020.

Van Breukelen, B.M., Rolle, M.: Transverse hydrodynamic dispersion effects on isotope signals in groundwater chlorinated solvents plumes, Environ. Sci. Technol., 46, 7700-7708, https://doi.org/10.1021/es301058z, 2012.

Van Breukelen, B. M., Prommer, H.,: Beyond the rayleigh equation: Reactive transport modeling of isotope fractionation effects to improve quantification of biodegradation, Environ. Sci. Technol., 42, 2457-2463, https://doi.org/10.1021/es071981j, 2008.

Vorosmarty, C., McIntyre, P., Gessner, M., Dudgeon, D., Prusevich, A., Green, P., Glidden, S., Bunn, S., Sullivan, C., Liermann, C., and Davies, P.: Global threats to human water security and river biodiversity, Nature, 467, 555–561, https://doi.org/10.1038/nature09440, 2010.

Walker, A.: A Simulation Model for Prediction of Herbicide Persistence, J. Environ. Qual., 3, 396–401, https://doi.org/10.2134/jeq1974.00472425000300040021x, 1974.

Wang, Y., Lai, A., Latino, D., Fenner, K., and Helbling, D.: Evaluating the environmental parameters that determine aerobic biodegradation half-lives of pesticides in soil with a multivariable approach, Chemosphere, 209, 430–438, https://doi.org/10.1016/j.chemosphere.2018.06.077, 2018.

Weiler, M.: Macropores and preferential flow-a love-hate relationship, Hydrol. Process., 31, 15–19, https://doi.org/10.1002/hyp.11074, 2017.

Weisner, O., Frische, T., Liebmann, L., Reemtsma, T., Ross-Nickoll, M., Schafer, R., Schaffer, A., Scholz-Starke, B., Vormeier, P., Knillmann, S., and Liess, M.: Risk from pesticide mixtures - The gap between risk assessment and reality, Sci. Total Environ., 796, https://doi.org/10.1016/j.scitotenv.2021.149017, 2021.

Wendell, A.K., Guse, B., Bieger K., Wagner, P.D., Kiesel, J., Ulrich U., Fohrer N.: A spatio-temporal analysis of environmental fate and transport processes of pesticides and their transformation products in agricultural landscapes dominated by subsurface drainage with SWAT+. Sci. Total. Environ., 945, 173629, https://doi.org/10.1016/j.scitotenv.2024.17362, 2024.

895   Wu, X., Li, M., Long, Y., Liu, R., Yu, Y., Fang, H., and Li, S.: Effects of adsorption on degradation and bioavailability of metolachlor in soil, J. Soil Sci. Plant Nut., 11, 83–97, https://doi.org/10.4067/S0718-95162011000300007, 2011.

Xu, Z., Liu, W., and Yang, F.: A new approach to estimate bioavailability of pyrethroids in soil by compound-specific stable isotope analysis, J. Hazard. Mater., 349, 1–9, https://doi.org/10.1016/j.jhazmat.2018.01.038, 2018.